Diploma Thesis

Evaluation of c-MET as a predictive marker for response to sorafenib in advanced hepatocellular carcinoma

submitted by

Peter Strobl

attaining the academic degree

Doktor der gesamten Heilkunde

Dr. med. univ.

at the

Medical University of Graz

conducted at the

Institute of Pathology, Medical University of Graz, Austria and

Division of Gastroenterology and Hepatology, **Department of Internal Medicine**, Medical University of Graz, Austria

under supervision of

Univ. Prof. Univ.-Doz. Dr. Carolin Lackner,

Univ. Prof. Dr. Rudolf Stauber and

Univ.-Ass. Dr. Stephan Jahn

Graz, 22.12.2016

Affidavit – Eidesstattliche Erklärung

I hereby declare that the following diploma thesis has been written only by the undersigned and without any assistance from third parties. Furthermore, I confirm that no sources have been used in the preparation of this thesis other than those indicated in the thesis itself.

Graz, 22.12.2016 Peter Strobl, eh.

Table of Contents

Abstract

Background and aims: Sorafenib is a multikinase inhibitor approved for the treatment of advanced stage hepatocellular carcinoma (HCC). However, its utility is impaired by development of resistance via activation of the met oncogene (c-MET) escape pathways. Treatment response may be related to the expression level of c-MET in HCCs. Furthermore, c-MET expression is also an important predictor of response to the c-MET inhibitor tivantinib, a potential second-line treatment for HCC. Expression of c-MET is usually assessed in a semiquantitative fashion using immunohistochemistry (IHC) and standardised evaluation criteria, a method prone to intra- and interobserver bias. C-MET expression can also be evaluated quantitatively using the mRNA in situ hybridisation assay RNA scope and digital image analysis (morphometry.) In our study, we first aimed to compare c-MET IHC and RNA scope for the assessment of c-MET expression. Second, we wanted to evaluate the utility of c-MET protein and RNA expression as prognostic and predictive markers for patients with advanced HCC.

Material and Methods: FFPE (formalin-fixed, paraffin-embedded) samples of 19 HCC patients, BCLC stages C and D, who received treatment with sorafenib were studied. Response to treatment was assessed using the modified response evaluation criteria in solid tumors (m-RECIST). C-MET expression in HCC tissue was assessed by IHC using the CONFIRM anti-Total c-MET antibody and with RNA scope. Protein and RNA expression was analysed semiquantitatively using light microscopy and numerical scores and quantitatively using digital image analysis. Response to treatment with sorafenib and survival of patient groups with low and high c-MET expression was compared by Kaplan-Meier method and log rank -test.

Results: The RNA Scope assay provided quantitative results comparable to the results obtained by semiquantitative IHC scoring. C-MET expression, regardless if measured quantitatively or semiquantitatively by IHC or RNA scope did not differ between patients responding versus those not responding to sorafenib. In addition, overall survival did not differ.

Conclusions: C-MET RNA scope is a valuable tool to minimize intra- and interobserver bias in the evaluation of c-MET expression in HCC. Contrary to previous research, this study did not find a difference in c-MET expression in respect to response to sorafenib in patients with advanced HCC.

Zusammenfassung

Grundlagen und Ziele: Sorafenib ist ein Kinaseinhibitor zur Behandlung von fortgeschrittenem Leberzellkarzinom (hepatocellular carcinoma, HCC). Jedoch sprechen Patienten häufig nicht auf das Medikament an oder entwickeln Therapieresistenz. Eine wichtige Rolle spielt dabei die Aktivierung von alternativen Signalwegen, die sich unter anderem durch die Überexpression von c-MET (met-Onkogen) zeigt. Die Expression von C-MET ist auch ein prädiktiver Wert für das Ansprechen auf Tivantib, das in der Behandlung von HCC Erfolge gezeigt hat. Die Expression von c-MET wird in der klinischen Routine mittels Immunhistochemie (IHC) untersucht und mit einem semiquantitativen Auswertungsschema dargestellt. Dabei treten jedoch Ungenauigkeiten durch eine wesentliche Intra- und Interobserver-Variabilität auf. Diese Probleme können vermieden werden, indem die Expression von c-MET mit einer mRNA In-situ-Hybridisierung (ISH) untersucht wird. Diese Methode liefert durch die Anwendung eines Bildanalyseprogramms (Morphometrie) auch quantitative Ergebnisse. Ziel dieser Studie war der Vergleich zwischen der in der Routinediagnostik verwendeten IHC und der neuartigen ISH-Methode RNA Scope. Weiters wurde der prädiktive und prognostische Wert der Expression von c-MET auf mRNA- und Proteinebene für das Therapieansprechen von Patienten mit fortgeschrittenem HCC und die Gesamtüberlebenszeit untersucht.

Material und Methoden: Es wurde das Formalin-fixierte, Paraffin-eingebettete (FFPE) Material von 19 Patienten, die zwischen 2007 und 2015 an der Klinik für Innere Medizin, Abteilung für Hepatologie und Gastroenterologie der Medizinischen Universität Graz aufgrund eines fortgeschrittenen HCCs mit Sorafenib behandelt worden sind, untersucht. Das Therapieansprechen wurde anhand von standardisierten radiologischen Kontrollen im Abstand von 3 Monaten bewertet. Die Expression von c-MET auf Proteinebene wurde mittels IHC (Antikörper CONFIRM anti-total c-MET) semiquantitativ bestimmt. Auf mRNA-Ebene konnte die Expression von c-MET durch die Verwendung von RNA Scope und Spot Studio, einer Software für digitale Bildanalyse, sowohl semiquantitativ als auch quantitativ bestimmt werden. Das Gesamtüberleben der Patientengruppen mit hoher und niedriger Expression von c-MET wurde mit der Kaplan-Meier-Methode und log-rank-Tests verglichen.

Ergebnisse: Die quantitativen Ergebnisse der c-MET Expression, bestimmt mit RNA Scope und automatischer Bildanalyse, stimmten mit den semiquantitativen Ergebnissen der IHC überein. Die Werte der c-MET-Expression auf Protein- und mRNA-Ebene von Patienten, die unter Therapie mit Sorafenib verlangsamtes Tumorwachstum zeigten und Patienten mit Tumorprogredienz unterschieden sich nicht. Bezüglich der Dauer des Gesamtüberlebens zeigten sich zwischen Patienten mit niedriger und hoher Expression von c-MET keine Unterschiede.

Schlussfolgerungen: Die Verwendung von RNA Scope kann die Ergebnisse der etablierten Methode IHC ergänzen und zur Vermeidung von Beobachter-assoziiertem Bias beitragen. Im Gegensatz zu den Ergebnissen früherer Studien konnten wir bei Patienten mit fortgeschrittenem HCC keinen prädiktiven und prognostischen Wert der Expression von c-MET auf mRNA- und Proteinebene für das Ansprechen auf Sorafenib und für das Gesamtüberleben darstellen.

Index of Abbreviations

AB	Antibody
AFLD	Alcoholic fatty liver disease
AFP	Alpha-Fetoprotein
AKT	Protein kinase B
ANGPTL1	Angiopoetin-like protein 1
ASH	Alcoholic steatohepatitis
BCLC	Barcelona clinic liver cancer classification
CEA	Carcino-embryonal antigene
CK	Cytokeratin
CT	Computertomography
c-MET	Met – protooncogene, hepatocellular growth factor receptor
CPS	Child-Pugh score
CR	Complete response
DAB	3,3'-Diaminobenzidin
DN	Dysplastic nodule
EASL	European association for the study of the liver
ECOG	Eastern cooperative oncology group performance scale
EGFR	Epidermal growth factor receptor
ERK	Extracellular signal–regulated kinase
FISH	Fluorescence in situ hybridization
FFPE	Formalin fixed, paraffin embedded tissue sample
HBV	Hepatitis B – virus
HCC	Hepatocellular carcinoma
HCV	Hepatitis C – virus
HE	Haematoxylin and eosin stain
HGF	Hepatocyte growth factor
HIF-1	Hypoxia inducible factor 1
HIV	Human immunodeficiency virus
HRP	Horseradish peroxidase
IGFR	Insulin-like growth factor receptor
IHC	Immunohistochemistry
ISH	In-situ-hybridisation

MAPK	Mitogen-activated protein kinases
MDB	Mallory-Denk body
m-RECIST	modified response evaluation criteria in solid tumours
MRI	Magnetic resonance imaging
m-RNA	Messenger ribonucleic acid
NBF	Neutral buffered formaldehyde
p-ERK	Phosporylated extracellular signal related kinase
PD	Progressive disease
PH	Portal hypertension
PDGFR	Platelet-derived growth factor receptor
PR	partial response
PI3K/AKT	phosphatidylinositide 3-kinases / protein kinase B (AKT) pathway
PT/INR	Prothrombin time/international normalized ratio
NAFLD	Non-alcoholic fatty liver disease
NASH	Non-alcolholic steatohepatitis
RFA	Radiofrequency ablation
RTK	Receptor tyrosin kinase
RN	Regenerative Nodule
SD	Stable disease
TACE	Trans-arterial chemoembolisation
TAGs	Triacylglycerides
TKI	Tyrosin kinase inhibitor
VEGFR	Vascular endothelial growth factor receptor
WHO	World health organization

Index of Figures

Index of Tables

1 Introduction

1.1 Anatomy of the liver

1.1.1 Macroscopic anatomy

The liver is the largest gland and inner organ in the human body. Its weight, approximately 1500g, accounts for 2% of the total body weight in adults. With the exception of the diaphragmatic area, the surface of the liver is covered by a serous membrane, the visceral peritoneum, which is smooth and shining. The porta hepatis, dividing the right from the left lobe of the liver, includes the portal vein, the hepatic artery and the common bile duct.[1] While macroscopic anatomy divides the liver into four lobes, Couinaud's classification system is based on the blood supply and divides the liver into segments (Table 1, Figure 1). Each of the eight segments has an independent blood supply as well as biliary duct system.[2] Therefore, surgical removal of individual segments is possible without interference with the blood flow and bile drainage in adjacent segments.

Figure 1: Couinaud´s segments of liver[1]

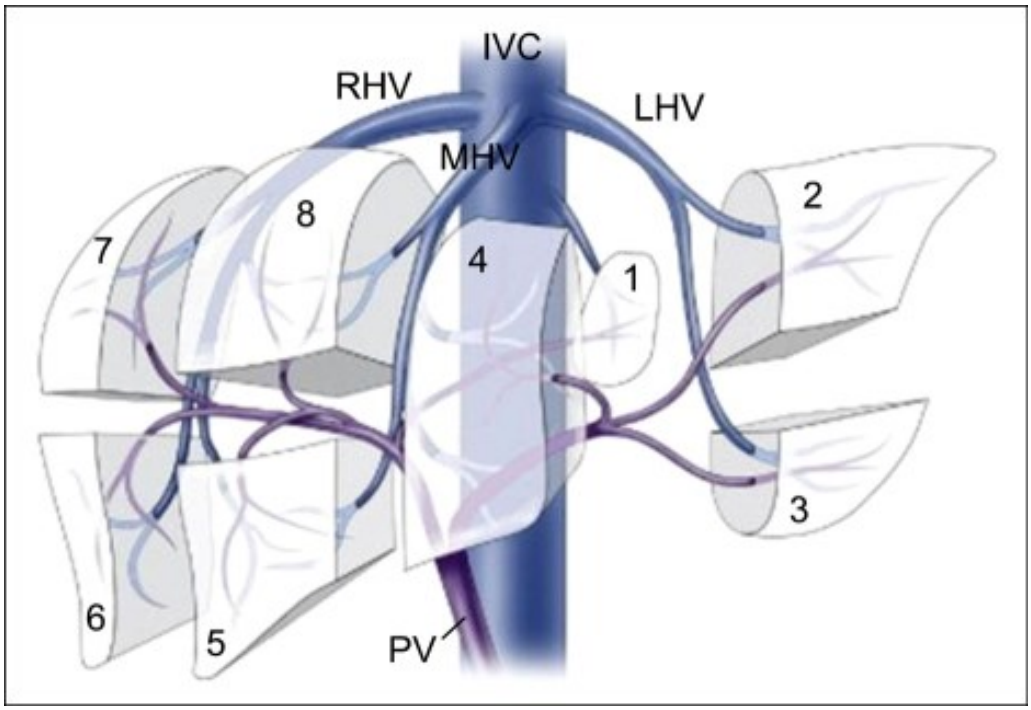

Table 1: Correspondence between anatomic lobes and Couinaud´s segments

Anatomic lobes	**Couinaud´s segments**
Left lobe - lobus caudatus	I
Left lobe – lateral segment	II, III
Left lobe – lobus quadratus	IVa, IVb
Right lobe – anterior segment	V, VIII
Right lobe – posterior segment	VI, VII

1.1.2 Microscopic anatomy

The liver tissue is composed of parenchymal cells, hepatocytes and non-parenchymal cells that have structural and immunologic functions. Table 2 provides an overview of the different cell types in the liver and their functions. The liver parenchyma is organized in lobules. In the center of the lobule there is the central vein while the portal tracts, containing a branch of the hepatic artery, portal vein and the bile duct (Glisson´s triad), are situated at the lobular periphery.[3]

The sinusoidal blood vessels stretch longitudinally from the central vein to the portal tracts. Between the sinusoids the hepatocytes form trabecular structures. The blood arriving from the intestine enters the liver in the portal vein and its branches and is distributed to the lobes and lobules together with the arterial blood supply via the hepatic artery. The fenestrated endothelium of the sinusoids allows an exchange of substances via the space of Dissé between the hepatocytes and the blood before it flows to the central and subsequently to the hepatic vein and the vena cava inferior.

Table 2: Hepatic cell types and their function[4]

Cell Type	Function
Hepatocytes	Parenchymal cells of the liver: Storage, synthesis, degradation of portal substances, metabolism, endocrine and exocrine functions
Sinusoidal endothelial cells	Fenestrated plexus facilitating contact of portal blood with hepatocytes
Kuppfer cells	Phagocytes of the liver, release of cytokines
Stellate cells	Function in regeneration following to injury, precursor to myofibroblasts
Cholangiocytes	Transport of bile, secretion of bicarbonate and water

1.2 Physiology

The liver serves major functions in the homeostasis and metabolism. These are reflected in the extensive blood supply, which equals 25% of the cardiac output.

Crucial functions of the liver are:

- The uptake of exogenous nutrients arriving from the intestinal tract via the portal vein.
- Synthesis, storage, modification and degradation of endogenous substances.
- Control of plasmatic concentration of metabolites and nutrients.
- Detoxification of toxic substances of endogenous and exogenous origin via biotransformation.
- Excretion of metabolites with the bile flow.

The metabolic functions of the liver are summarised in Table 3.[5]

Table 3: Metabolic functions of the liver

Carbohydrate metabolism	• Uptake of glucose, fructose and galactose from the portal venous blood. • Synthesis of glucose from other carbohydrates. • Storage of glycogen and release of glucose in a catabolic state. • Gluconeogenesis: synthesis of glucose to maintain blood glucose level in a katabolic state
Lipid metabolism	• Transformation of glucose to triacylglyerides • Synthesis of ketone bodies from fatty acids • Synthesis of cholesterol and lipoproteins
Protein metabolism	• Synthesis of liver-specific enzymes • Synthesis of serum proteins: albumin, coagulation factors etc. • Synthesis of acute-phase proteins: C-reactive protein, complement factors, Alpha 1-antitrypsin
Elimination and detoxification	• Degradation of haemoglobin, synthesis of bilirubin • Synthesis of bile acids and secretion of bile into the duodenum. • Uptake of xenobiotic substances such as drugs, glucuronidation and excretion via bile • Degradation of ethanol to acetyl-CoA
Endocrine balance	• Synthesis of hormones: Angiotensiogen. • Activation of hormones: Calcidiol • Inactivation of steroid hormones

1.3 Cirrhosis

The World Health Organisation (WHO) defines cirrhosis as a diffuse process characterized by the formation of fibrous septa and the conversion of the normal liver architecture into structurally abnormal nodules. Cirrhosis is the common end stage of many chronic liver diseases.[6]

1.3.1 Aetiology and epidemiological aspects

Cirrhosis is most satisfactorily classified by its aetiology, since the morphologic outcomes of end-stage liver diseases are highly variable. Morphologic features may point towards a possible aetiology, but once cirrhosis is fully established, it is frequently impossible to make an aetiological diagnosis on morphologic grounds alone.[7]

Figure 2: Causes of cirrhosis in the Western European population[8]

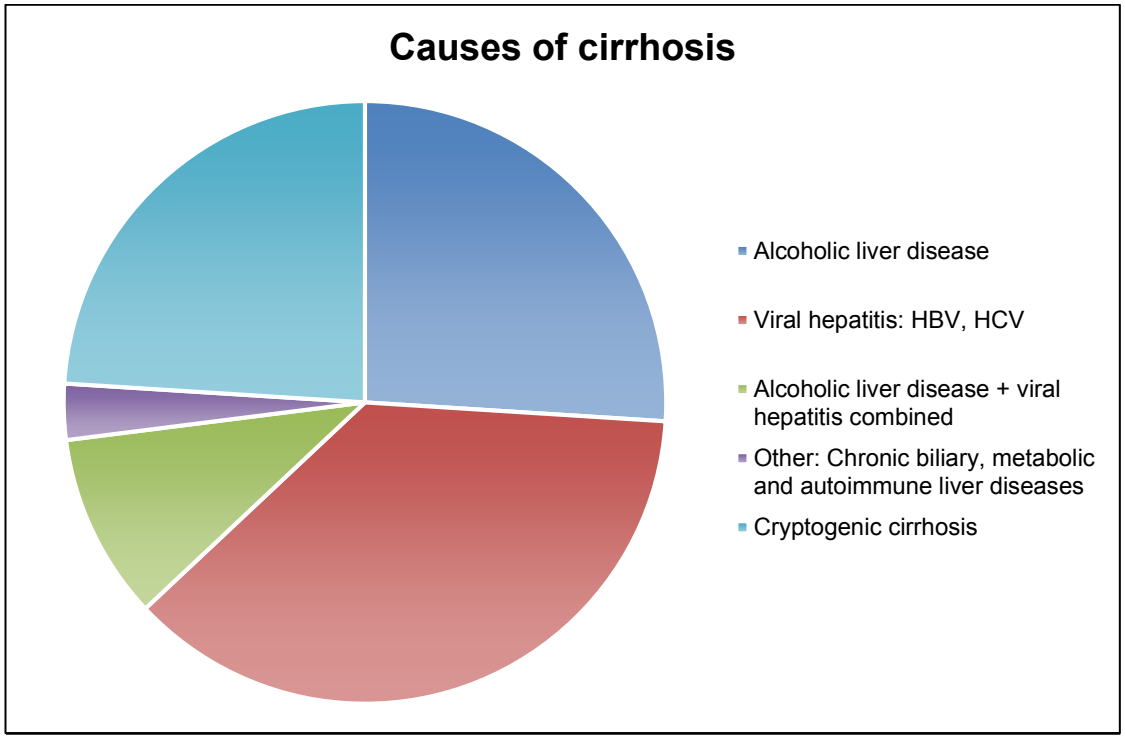

The causes of cirrhosis differ between geographic regions and social groups. Hepatitis B virus (HBV) has the highest prevalence in South East Asia, Africa and South America. Approximately 8% of the world´s population are carriers of HBV, which can be conducted by blood and semen.[9] Around 3% of the world´s population

are infected with Hepatitis C virus (HCV). In the past decades, contamination of blood product was the leading cause of HCV infection. However, this route of infection is no longer relevant as a consequence of the introduction of sensitive screening tests for blood products for HCV. Autoimmune processes such as autoimmune hepatitis and the chronic biliary liver diseases, primary sclerosing cholangitis (PSC) and primary biliary cholangitis (PBC) are rare in the global population but higher prevalences are found in in certain ethnic groups.[10] Non-alcoholic fatty liver disease (NAFLD), mostly related to the liver manifestation of the metabolic syndrome is the most common chronic liver disease in populations with Western lifestyle. In the US and Europe, the estimated prevalence of NAFLD in the population ranges between 17 to 33%.[11] NAFLD is nowadays considered to be among the most frequent cause of cirrhosis.[12] Another important cause of fatty liver disease and cirrhosis besides the metabolic syndrome, is alcohol abuse causing alcoholic fatty liver disease (AFLD).[13]

1.3.2 Pathogenesis of cirrhosis

Liver cirrhosis is a dynamic process of progressive fibrosis of the parenchyma and distortion of the normal histological architecture. The trigger of this process is a complex interplay between injury and endogenous response-to-damage. The central pathologic mechanism is cell death, which initiates regeneration and fibrosis[14]. Type I and III collagen are components of fibrous septa which destroy the liver lobular architecture. In addition, the sinusoids are converted into capillaries resting on a continuous basement membrane which impairs the exchange of substances between the portal blood and the hepatocytes.[15]

1.3.3 Morphology of cirrhosis

Cirrhosis used to be divided into micronodular and macronodular forms. However, the size of the nodules is influenced by mechanisms of regeneration and liver injury. Hepatic injury acting predominantly at the lobular level frequently results in micronodular cirrhosis. The ratio of collagenous matrix to parenchyma is increased, causing an increased organ consistency. In early stages and certain aetiologies, the size of the liver can be increased while with in later stages of cirrhosis with advancing loss of parenchyma the organ size decreases and consistency increases.

In macronodular cirrhosis, large parenchyma nodules containing several portal tracts are separated by dense fibro-vascular septa. Macronodular cirrhosis may transform into the micronodular form in cases with ongoing activity of the underlying liver disease.[16] Morphological features of cirrhosis may indicate aetiology (see Table 4).

Table 4: Pattern of cirrhosis

	Micronodular cirrhosis	**Macronodular cirrhosis**
Underlying disease	AFLD, NAFLD, Hemochromatosis, Wilson´s disease	Viral hepatitis (HBV/HCV), Autoimmune hepatitis
Size of nodules	< 3mm	>3mm
Size of organ	Early stage: enlarged; Advanced stage: de-creased size	Enlarged

1.3.4 Clinical management and complications of cirrhosis

Clinical symptoms of cirrhosis include fatigue, weight loss, misbalance of hormones because of alterations in the steroid metabolism and cutaneous conditions such as telangiectasia and palmar erythema. The increased flow resistance of the cirrhotic liver results in portal hypertension causing varicosis of the oesophagus, ascites, oedema and enlargement of the spleen. Clinical signs indicating decompensation of cirrhosis are icteric skin, haemorrhagic diathesis and hepatic encephalopathy.[17]

The Child-Pugh score (CPS) is used to estimate the prognosis of patients with cirrhosis using five clinical measures. The points of the CPS are added to classify Child-Pugh-class A to C.[18] Tables 5 and 6 illustrate the calculation of Child-Pugh classes and their prognostic impact.

Table 5: Child-Pugh score

Measure	1 point	2 points	3 points
Total bilirubin (md/dl)	<2	2-3	>3
Serum albumin (g/dl)	>3.5	2.8-3,5	<2.8
PT INR	<1.7	1.71-2.3	>2.8
Ascites	None	Mild	Moderate-severe
Hepatic encephalopathy	None	Grade I-II	Grade II-IV

Table 6: Calculation of Child-Pugh classes:

Child-Pugh class	Points	1-year-survival
A	5-6	Nearly 100%
B	7-9	85%
C	10-15	35%

The treatment options of cirrhosis are aimed at the control of the underlying liver disease like viral hepatitis, metabolic syndrome or chronic alcohol abuse and the prevention of complications. Because cirrhosis is a risk factor for the development of HCC, patient should be included in appropriate screening programmes.[19] Currently, ultrasonography is the most widely used method in screening for HCC. Studies showed contradictory results for the optimal interval of ultrasonography examinations for the reliable detection of HCCs. Alpha-Fetoprotein (AFP) is a biomarker expressed by foetal hepatocytes and HCC cells. Although AFP is used as a tumormarker for HCC in clinical practice its utility is impaired by a low sensitivity.[20]

1.4 Hepatocellular carcinoma

HCC is defined as a malignant tumor with hepatocellular differentiation.[21]

1.4.1 Aetiology and epidemiology

Cancer of the liver is the sixth most common cancer and is the third cause of cancer related deaths worldwide. HCC accounts for 90% of primary liver cancers. HCC occurs in the majority of the cases in a fibrotic, frequently cirrhotic liver. The prevalence of HCC has been increasing progressively with advancing age in all populations with a peak at 70 years due to the rising prevalence of viral infection-, toxic (ethanol)- and/or metabolic syndrome-associated cirrhosis [22] In developing countries, the exposure to Aflatoxin B1 of Aspergillus flavus and A. parasiticus is an important co-factor for the development of HCC in patients with chronic hepatitis B virus infection.[23] In almost all populations, males have higher rates of HCC prevalence than females, with ratios between 2:1 and 4:1. The reason for this may be partly explained by gender-specific differences in exposure to risk factors.[24]

1.4.2 Macroscopy

The frequently encapsulated tumors show soft consistency and a yellow-green colour. Depending on the size and/or therapeutic intervention necrotic areas can be seen. Both unifocal and multifocal forms of HCC occur. In the case of multifocality, neoplastic tumor nodules are distinctly separated by non-neoplastic tissue. Unifocal HCCs grow as a single nodule or form clusters of coherent nodules while multifocal HCCs arise simultaneously in the cirrhotic liver. Alternatively, they may represent the result of intrahepatic tumor spread. The cirrhoto-mimetic HCC is a rare growth pattern characterised by invasive growth of small tumor nodules within cirrhotic liver tissue.[25] Tumor spread occurs via lymphatic and haematogenous routes. Most common sites of extrahepatic spread are the lungs, lymph nodes, bones and adrenal glands.[26]

1.4.3 Histopathology

The trabecular pattern is the architectural pattern most frequently encountered. The tumor trabeculae are formed by several (>2) layers of tumor cells. The thickness of the trabeculae increases with increasing degree of dedifferentiation. The pseudoglandular or acinar pattern shows gland-like structures of single tumor cell layers around abnormal bile canaliculi. Within these structures, bile can be present. Pseudoglandular structures often occur together with the trabecular pattern. The compact pattern is a feature of poorly differentiated HCCs. Here, the blood spaces appear very narrow giving the tumor the appearance of a solid mass.[27]

The HCC tumor cells resemble normal hepatocytes. Usually they are smaller with enlarged polymorphic and hyperchromatic nuclei and basophilic polygonal cytoplasm. However, the tumor cells frequently exhibit cytoplasmic changes and/or inclusions which may also lead to an increase tumor cell size, like ballooning degeneration, fatty change or microvesicular steatosis. Ballooned tumor cells frequently contain hyaline bodies. Mallory Denk bodies (MDBs) frequently occur in ballooned tumor cells whereas intracytoplasmic hyaline bodies are found in non-ballooned tumor cells. Tumor cell ballooning, MDBs, fatty change and intratumoral inflammation as well as pericellular fibrosis are features of the so-called steatohepatitic variant of HCC. Pale bodies consist of fibrinogen. Clear cell change may be the result of glycogen storage in HCC cells. Pleomorphic and multinucleated tumor cells are commonly found in poorly differentiated tumors. MDBs may be abundant in fibrolamellar type of HCC. Sinusoid-like blood vessels (sinusoid equivalents) form the sparse stroma between the tumnor cell trabeculae, but abundant fibrous stroma between trabecular and/or pseudoglandular tumor cell structures is uncommon. The endothelial cells differ from the normal endothelium of sinusoids: They resemble non-fenestrated endothelium of capillaries with expression of markers like CD34 and they lack expression of CD31 as in regular sinusoidal endothelium. 90% of HCCs show a positive immunohistochemical staining with the marker HepPar1, a marker of hepatocellular differentiation. HCC cells typically show a membranous staining pattern with polyclonal antibodies against the canalicular marker carcino-embryonal antigene (CEA). Other markers

albeit of low sensitivity and specificity include AFP and the cytokeratins CK8 and CK18.[25]

There is a great variety in the histomorphological features among different HCCs as well as within the same tumor. The intratumoral heterogeneity may be explained by a step-by-step dedifferentiation resulting in a so-called nodule-in-nodule phenomenon in which smaller nodules of less well differentiated morphology arise in larger nodules with higher grade of differentiation.[28]

Several types of HCC differ from classical HCC. The fibrolamellar subtype shows different histology, molecular biology and occurs in non-fibrotic livers of children and young adults. Characteristic feature of fibrolamellar HCC are laminated fibrous layers between large polygonal tumor cells with abundant eosinophilic cytoplasm. Scirrhous HCCs show fibrosis along the sinusoid-like blood spaces and atrophy of the tumor cell layers. Sclerotic changes in HCC may also result from therapeutic measures e.g. trans-arterial chemoembolisation (TACE). Table 7 gives a summary of histological grading of HCC, which is based on cellular atypia and architectural pattern.[29]

Table 7: Histological features and grading of HCC

Grading	**G**	**Cytological features**	**Architectural pattern**
well-differentiated HCC	G1	Mild cellular atypia, frequently fatty change	Thin trabecular pattern
Moderately diff. HCC	G2	Abundant cytoplasm, round nuclei, distinct nucleoli	Trabecular growth of 3 or more cells, pseudoglandular pattern
Poorly diff. HCC	G3	Increased nucleus-to-cytoplasm ratio, moderate to strong pleomorphism	Solid pattern
Undiff. HCC	G4	Spindle-shaped or round cells, little cytoplasm	Solid pattern

1.4.4 Differential diagnosis and precursor lesions of HCC

Table 8 provides an overview on liver tumors of hepatocellular differentiation, some of which may be precursor lesions of HCC (for HCC, see chapers 1.2.2 and 1.2.3).[30,31]

Table 8: Morphology and histology of tumors of hepatocellular differentiation

Nomenclature	**Hepatocellular adenoma (HCA)**	**Focal nodular hyperplasia (FNH)**	**Dysplastic nodule (DN)**
Morphology	Commonly solitary, globular mass of up to 3000g, frequently haemorrhage or necrosis	Singular or multiple nodules, central scar with fibrous septa stretching to periphery	Nodular foci of dysplasia in cirrhotic liver
Histology	Hepatocytes in plates of 2-3 layers, separated by normal sinusoids, dysplasia may be present	Localised region of hyperplasia in a normal liver, no cellular atypia	Hepatocytes featuring atypia of various grade, stromal invasion may be present
Malignant potential	Benign lesion without adenoma carcinoma sequence	Benign lesion, no risk of transformation	Precancerous lesion of HCC
Clinical aspects	Arises in normal liver, association with oral contraception or steroid intake, female predominance	Arises in normal liver, association with oral contraception or steroid intake, female predominance	Arises in cirrhosic tissue

Focal nodular hyperplasia (FNH) and hepatocellular adenoma (HCA) typically occur in non-fibrotic liver tissue of females and are correlated with the intake of oral contraceptives containing estrogens. These benign lesions can be distinguished with imaging methods such as duplex sonography and magnetic resonance imaging

(MRI) in many cases. However, histology plays an important role in lesions with atypical presentation.[32]

Precancerous lesions of HCC occur in cirrhotic or fibrotic but only rarely, in non-fibrotic liver as foci of cellular dysplasia at the microscopic level, and as nodular lesions, dysplastic nodules (DN), detectable in imaging and in macroscopic examination. According to their grade of cellular and architectural atypia, DN are divided in low grade and high grade lesions. Tumor neoangiogenesis is a central step and is increasing during the development from DN to HCC. The criteria for classification of nodular precursor lesions of HCC in cirrhotic liver are described in Table 9.[32]

Table 9: Classification of benign precursor lesions and HCC in cirrhotic liver

Feature	**RN***	**Low grade DN****	**High grade DN**	**Well-diff. HCC**	**Moderately diff. HCC**
Anatomical change	portal tracts are present	Portal tracts are present, no unpaired arteries	Portal tracts and unpaired arteries	Blood supply: unpaired arteries, remnant portal tracts entrapped in periphery of HCC	Blood supply by unpaired arteries
Stromal invasion	Absent	absent	present	present	present
Gross appearance	Nodular	nodular	nodular	nodular	Distinctly nodular
Arterial supply	unequal; tissue reaction to heterogeneous blood supply	Iso/ hypovascular	Iso/ hypovascular	Iso/ hypovascular, rarely hypervascular	hypervascular
Classification	benign	premalignant	premalignant	Early HCC	Progressed HCC

*= Regenerative nodule,
**=Dysplastic nodule

1.4.5 Staging systems

The purpose of staging systems is prediction of outcome and patient stratification in order to guide individualized patient management. The main variables contributing to HCC staging are tumor size and number, liver function, and clinical performance status. The staging system recommended by the European association for the study of the liver (EASL) is the Barcelona clinic liver cancer classification (BCLC, Figure 3). Molecular classification of HCC based on gene signatures or molecular abnormalities has been described. However, such a system is not yet available for clinical application.[33]

Figure 3: BCLC classification of HCC and treatment strategy[3]

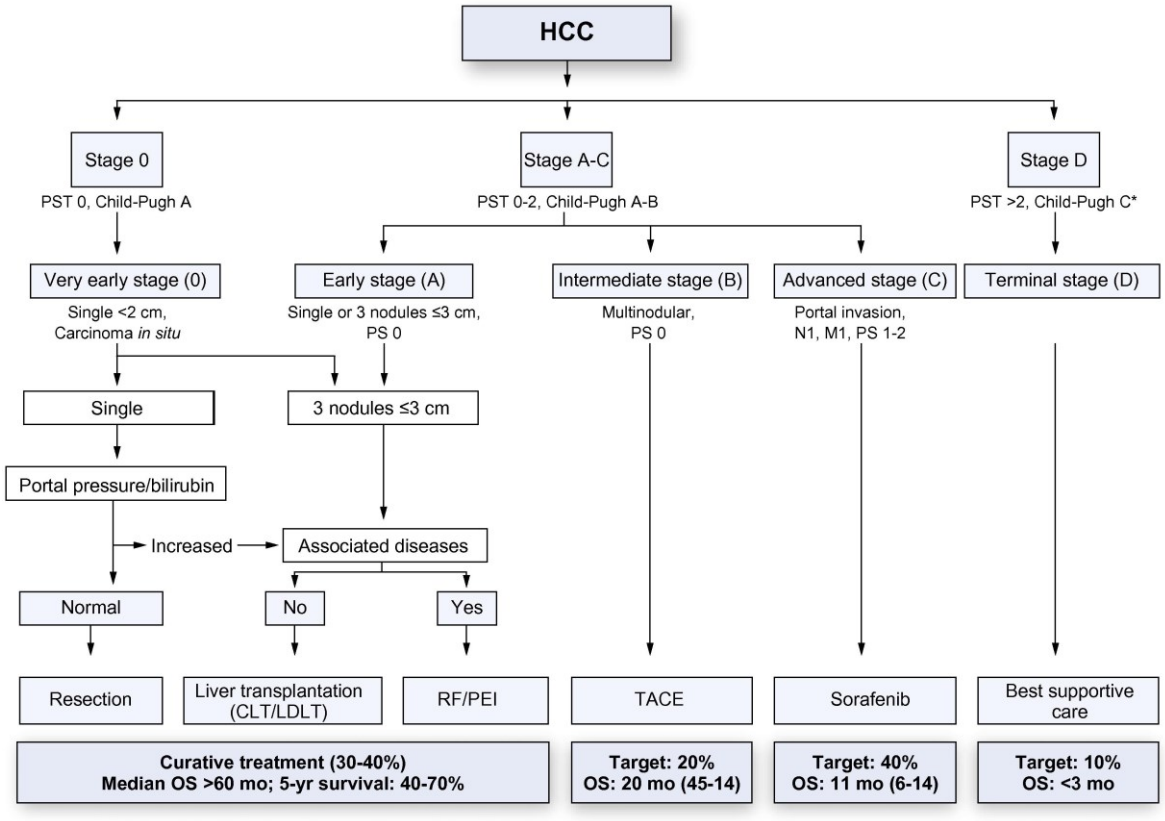

Figure 3: The assignment of treatment for patients with HCC depends on tumor stage, stage of cirrhosis (CPS), performance status (PST) and associated diseases. If HCC is diagnosed at an early stage, curative treatment options such as resection and liver transplantion are available with median overall survival (OS) of >60 months. With advanced tumor stage, OS declines rapidly.

The conventional TNM system (see Table 10) is not of major significance for treatment decisions. It is defined by variables related to tumor size, number, vascular invasion and evidence of metastatic spread. It has been mostly tested by HCC patients in the surgical setting. The prognostic value seems to be limited.[34]

Table 10: 7th edition of UICC TNM classification for HCC[35]

T – Primary tumor	
Tx	Primary tumor cannot be assessed
T0	No evidence of primary tumor
T1	Solitary tumor without vascular invasion
T2	Solitary tumor with vascular invasion or multiple tumors, none > 5 cm
T3a	Multiple tumors > 5 cm
T3b	Single tumors or multiple tumors, invasion of hepatic or portal vein
T4	Tumor(s) with direct invasion of adjacent organs other than gallbladder or with visceral peritoneum
Regional lymph nodes (N)	
Nx	Regional lymph nodes cannot be assessed
N0	No Regional lymph nodes metastasis
N1	Regional lymph nodes metastasis
Distant metastasis (M)	
M0	No distant metastasis
M1	Distant metastasis

1.4.6 Clinical management

Patients with HCC may present with hepatic decompensation and ascites and/or paraneoplastic symptoms such as hypoglycaemia and hypercalcaemia. The tumor shows a high potential of vascular invasion. Tumor dissemination is via the haematogenous and lymphatic route. HCC are insensitive to radiotherapy and refractory to cytotoxic chemotherapy.[36] Overall survival (OS) decreases significantly with advanced tumor stage.

Curative treatment options are only indicated for early stages and include resection, local ablative methods (radiofrequency ablation) and liver transplantation (see table 5). Resection is the first line option for patients with a solitary tumor and good liver

function as indicated by stage A according to the BCLC system. Liver transplantation is reserved for patients with a tumor/tumors of smaller size as defined by the Milan criteria who are not suitable for resection. If transplantation is not possible for clinical reasons, radiofrequency ablation or TACE may be indicated.[37]

At the moment, the only systemic treatment option available for advanced stages of HCC in clinical practise is targeted therapy using the multi-tyrosin-kinase inhibitor (TKI) sorafenib. Other drugs are being developed and are only used in clinical trials. An example is the selective inhibitor of the hepatocyte growth factor receptor (c-MET oncogene) tivantinib which was related to improved survival in a phase II randomized, placebo controlled trial of patients with progressive HCC.[38] The beneficial effect of tivantib may not only be based on inhibition of c-MET, but also on a non-MET dependent cytotoxic effect.[39]

1.4.7 Sorafenib: A treatment option for advanced HCC

Sorafenib is a TKI which directly inhibits kinases with oncogenic attributes such as RAF proto-oncogene serine/threonine-protein kinase (C-Raf) and B-Raf, the pro-angiogenic receptor tyrosin kinase (RTK) vascular endothelial growth factor receptor (VEGFR) and platelet-derived growth factor receptor (PDGFR), tyrosine kinases such as the KIT proto-oncogene receptor TK (c-kit) and the phosphorylated extracellular signal related kinase (p-ERK). These proteins are involved in tumor progression, invasiveness and angioneogenesis.[40]

According to the EASL guidelines, sorafenib is the first line treatment option for patients of BCLC stage C, CPS A-B and Eastern cooperative oncology group (ECOG) Performance Status 1-2.[41] Results of several clinical studies showed that median survival and the time to radiologic progression were nearly 3 months longer for those who were treated with sorafenib than for those given placebo.[42] Infrequently, patients may show complete tumor remission.[43,44]

Nevertheless, patients in considerable numbers have progressive disease under treatment and have to be considered non-responders. Adverse effects may occur in

80% of cases treated with sorafenib [47]. Adverse effects can be severe and include fatigue, weight loss, dermatologic symptoms such as alopecia and hand-foot skin reaction, gastrointestinal symptoms such as diarrhoea, nausea and hypertension. The decreased effect of sorafenib after initial satisfying response may be explained by the activation of escape pathways.

1.4.8 Function of c-MET in HCC

C-MET acts as the receptor for hepatocyte growth factor (HGF) and is essential for liver development and response mechanisms to liver damage.[45] In the cancer setting, the HGF/c-MET axis promotes tumorgenesis by stimulating cell proliferation, survival, motility, invasion and angiogenesis.[46] C-MET activates the ERK/MAPK pathway and the phosphatidylinositol 3-kinase / protein kinase B (PI3K/AKT) pathway as illustrated in Figure 4.

Mitogen-associated protein kinases (MAPKs) regulate various cellular processes such as proliferation, differentiation, stress response, apoptosis and survival. Extracellular stimuli via mitogens, cytokines and growth factors like HGF stimulate the activation of the MAPKK kinase (MAPKKK) c-MET. Eventually, signalling via the MAPKKs follows a three-tiered kinase cascade: MAPKKK > MAPKK > MAPK. Finally, activated MAPKs phosphorylate and activate specific protein kinases (MAPKAPK), which amplify and mediate the cellular functions regulated via the MAPK pathway.[47]

Another pathway regulated by c-MET is the PI3K/AKT – pathway. Akt is a kinase regulating cell survival, proliferation and growth. This pathway is activated by extracellular signals such as growth factors and is amplified via the lipid kinase PI3K, which induces the activation of Akt via PIP3. For its effects on proliferation and inhibition of apoptosis, Akt is considered a proto-oncogene.

Figure 4: C-MET signalling in HCC[48]

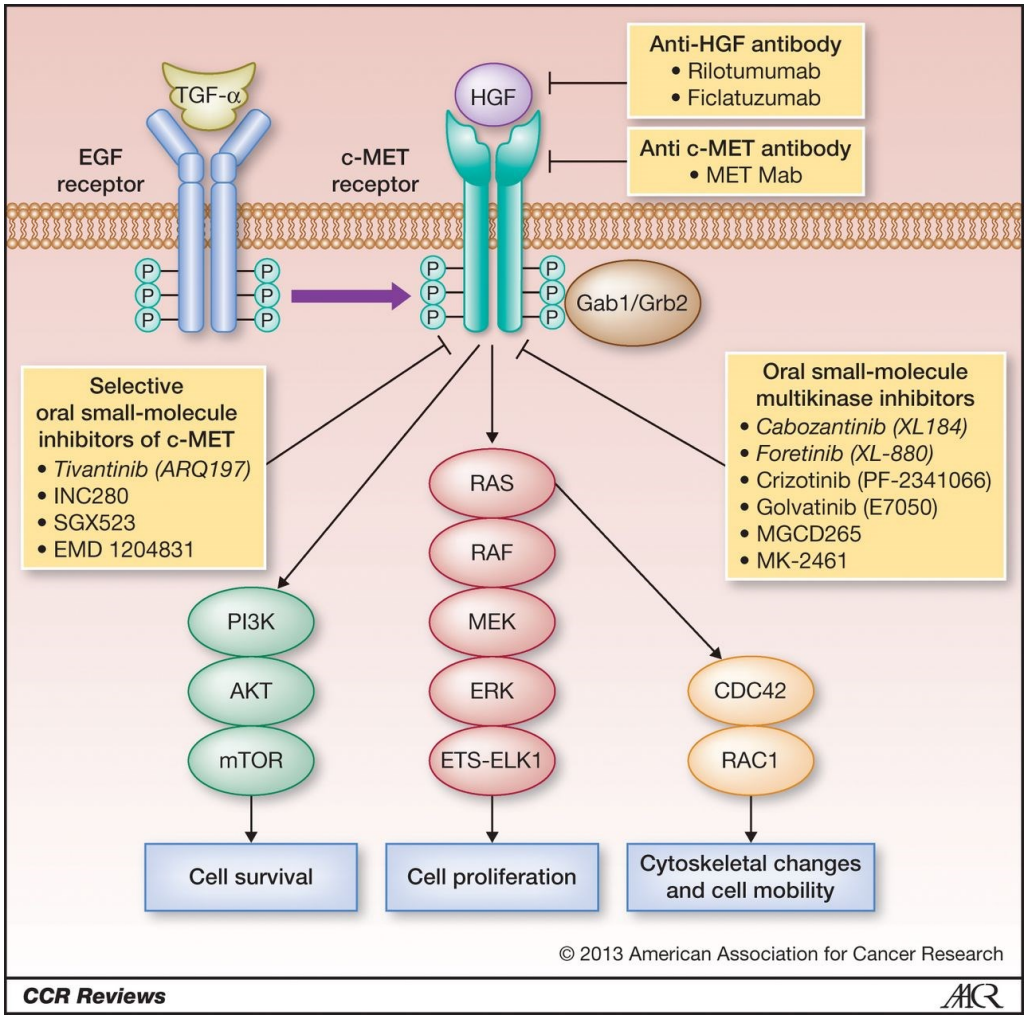

Figure 4: Pathways regulated by c-MET as an upstream cytomembranous receptor and various therapeutic approaches, of which c-MET inhibitor tivantinib is most promising as a second line treatment for advanced HCC.

Aberrant expression of c-MET has been detected in tumors of various origins such as in non-small cell lung cancer, where it promotes chemoresistance and radioresistance by inhibition of apoptosis via activation of the PI3K-AKT pathway.[49] Several studies investigated the status on c-MET in HCC. C-MET overexpression has been found was found frequently in tumor tissue and correlated with poor to moderate tumor differentiation, increased incidence of intrahepatic metastasis and shorter recurrence-free survival. Previous research reports rates of c-MET overexpression of up to 100% in HCC tissue while gene amplification was found less frequently.[50,51,52] The high rate of overexpression of c-MET overexpression provides a rationale to use inhibitors of c-MET and downstream components of pathways regulated by c-MET for the treatment of HCC.

1.4.9 C-MET and sorafenib resistance

Tumor neoangiogenesis and hypervascularisation represents an important step in development of HCC. During malignant transformation of DN, there is an increase of arterial blood supply through the formation of so called unpaired arteries (arterial branches of the hepatic artery not accompanied by portal vein branches and interlobular bile ducts) (see also Table 6).

Hypervascularisation of HCC seems to be associated with a moderate to poor tumor differentiation grade. Patients with high degree of hypervascularisation have a higher percentage of recurrence after resection compared to those with lower vascularisation grade.[53] Increased expression of markers related to angiogenesis such as angiopoietin-2 and CD34 further underline the role of angiogenesis as a driving force in HCC development.[54] The anti-angiogenic effect of sorafenib relies on inhibition of the RAF/MEK/ERK pathway via the RTKs VEGFR and PDGFR. The interplay between pathways contributing to angiogenesis is complex. Hence, the redundancy of angiogenetic mechanism may contribute to resistance to sorafenib by activation of alternative pathways.[55]

Beside angiogenesis via RTKs, hypoxia is another trigger of invasive growth in HCC. It has been proposed that hypoxia caused by inhibition of angiogenesis could trigger invasive signaling pathways, which could explain the modest clinical benefits with respect to progression free and overall survival under treatment with anti-angiogenic drugs such as sorafenib.[56] Low oxygen concentration in HCC tissue induces expression of factors like hypoxia inducible factor 1 (HIF-1). HIF-1 is a transcription factor which activates angiogenesis, via alternative pathways like c-MET signaling. In HCC, HIF-1 (subunit α) triggers epithelial-mesenchymal transformation (EMT) and facilitates invasion and metastasis.[57] HIF-1 also enhances transcription of c-MET RNA (ribonucleic acid) and expression of c-MET protein. Hence, hypoxic tumor regions may be characterized by upregulation of c-MET.

Anti-angiogenic therapies may interfere with c-MET activation in a dual way:

(1) By enhanced expression of c-MET inducted by hypoxia and

(2) By promoting c-MET signalling as a consequence of VEGFR blockade.[58]

This hypothesis is supported by in-vitro experiments showing overexpression of c-MET in cell lines with low baseline expression after long-term treatment with sorafenib while c-MET inhibition reversed the capability of invasion and migration[59]. Another in-vitro study showed that sorafenib resistance can be induced by activation of the c-MET pathway via administration of hepatocyte growth factor (HGF) in the serum.[60]

In summary, c-MET may play a crucial role in tumor escape from hypoxia caused by anti-angiogenic therapy. Understanding this interplay between therapy and tumor reaction may help to overcome sorafenib resistance and improve survival of patients with advanced HCC.

2 Hypothesis

We hypothesize that

- Low expression of c-MET in HCC tumor tissue as detected by IHC (immunohistochemistry) and RNA Scope correlates with response to treatment with sorafenib, resulting in prolonged overall survival.
- High expression of c-MET in tumor tissue will identify patients likely to develop resistance against sorafenib and suffer shorter survival.

3 Objectives

The fact that there are significant differences in the response patterns among HCC-patients treated with sorafenib implies the need to identify predictive markers as well as to improve the understanding of the mechanisms involved in resistance to sorafenib. Despite considerable scientific efforts, no universally accepted predictive marker is available in clinical practise. The identification of markers for the prediction of response of patients with HCC to treatment with sorafenib will be a major asset in patient management. Non-responders can be identified and saved from unnecessary treatment and side effects.

4 Goals

- We will evaluate and compare the assessment of C-MET expression in formalin-fixed, paraffin-embedded (FFPE) HCC tissue in 19 patients with advanced stage HCC by IHC and RNA Scope and semi-quantitative and quantitative scoring.
- C-MET protein and mRNA expression will be correlated to tumor response classes according to the modified response evaluation criteria in solid tumors (mRECIST) and to length of overall survival.

5 Methods

5.1 Patient recruitment

For this retrospective pilot study we recruited 69 patients with diagnosis of advanced-stage HCC who had undergone a tumor biopsy for the histological diagnosis of HCC and who had received sorafenib as a palliative therapy. The patients were treated between 2007 and 2015 at the Division of Gastroenterology and Hepatology of the Medical University of Graz. According to the EASL guidelines, the patients were classified as BCLC C (advanced stage) with cirrhosis of Child-Pugh class A and B. Cases with biopsies of insufficient quality were excluded. Furthermore, we excluded patients who were lost to follow-up. We finally identified 19 patients who fulfilled the inclusion criteria of the study as mentioned above. Figure 5 gives a summary of the steps of patient recruitment in this study. FFPE biopsy material was obtained from the biorepository of the Medical University of Graz (Biobank Graz). Informed consent was obtained for each patient. The study was approved by the Ethical Review Committee of the Medical University of Graz (EK 27-036 ex 14/15).

Figure 5: Patient recruitment process

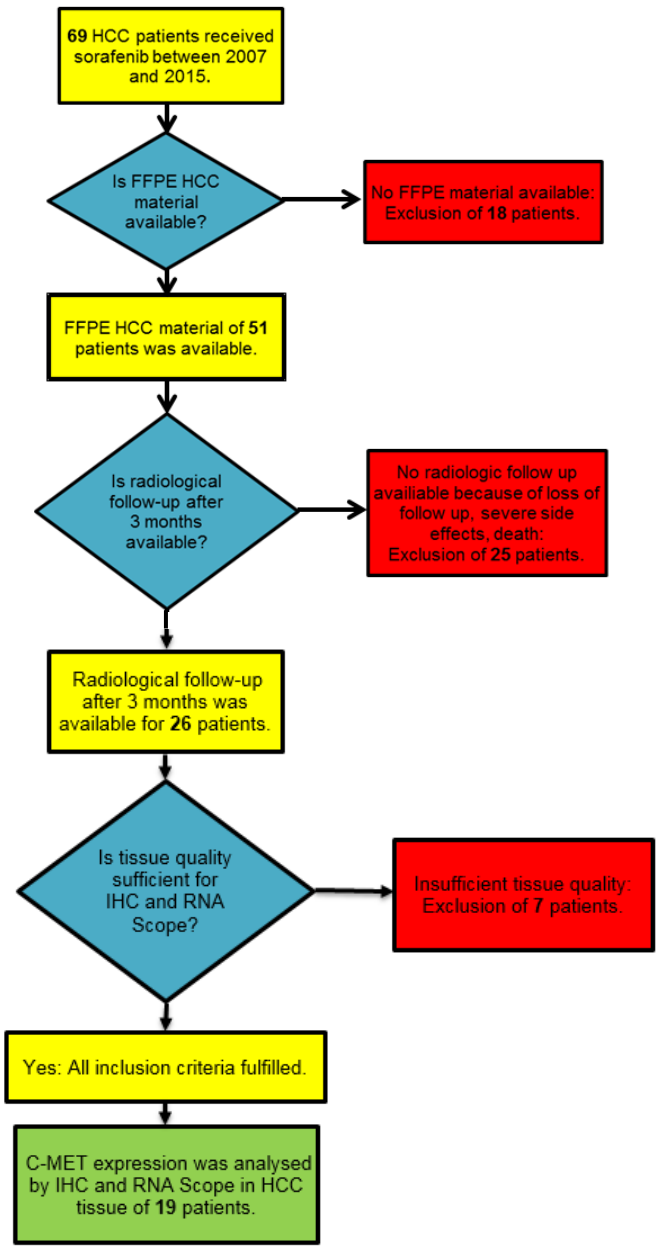

Figure 5: Flowchart table summarising the steps of patient recruitment.

5.2 Radiological assessment of response to sorafenib

The assessment of response to treatment is a pivotal aspect of studies on antineoplastic therapy. Guidelines for reporting response in clinical studies are the subject of a continuously evolving process which is influenced by the development of novel therapeutic agents as well as the development of new imaging techniques. In the late 1970s, the WHO guidelines on the interpretation of results of cancer treatment were established. The aim was to develop a “common language” for describing these results and to agree on general principles for reporting and assessing data.[61] Categories of objective response were defined as complete response (CR), partial response (PR), no change / stable disease (SD) and progressive disease (PD). Basic principle for this classification is the observation of a decrease or increase of the tumor area or of the tumor measured in a linear dimension.

The RECIST (response evaluation criteria in solid tumors) classification, published in 2000, keeps the basic categories of CR, PR, SD and PD and gives precise instructions on assessment of overall tumor burden and evaluation of target lesions and non-target lesions. Target lesions (up to five per organ) are defined by their size and their suitability for repeated measurements. All other lesions should be assessed as non-target lesions. RECIST considers technical progress in imaging and recommends computer tomography (CT) and magnet resonance imaging (MRI) scans as a primary imaging modality.[62]

However, treatment of HCC such as locoregional therapies and molecular-targeted therapies may not decrease the size of the tumor itself but instead decrease the burden of viable tumor tissue by inducing necrosis. Hence, the modified RECIST (m-RECIST) assessment, a set of guidelines for studies on HCC was developed. One principal point is the concept of measuring viable tumor tissue. Viable tumor is defined as uptake of contrast agent in the arterial phase of dynamic CT or MRI. In m-RECIST (as in the conventional RECIST) overall patient response combines target lesion response, non-target lesion response and emergence of new lesions.

These m-RECIST criteria are summarized in Tables 11-12. The tumor response to treatment has to be evaluated against the sum of the diameters of viable tumor tissue at baseline.[63]

Table 11: mRECIST assessment of target lesion response

Complete response	**CR**	Disappearance of any intratumoral arterial enhancement in all target lesions
Partial response	**PR**	>30% decrease in the sum of diameters of viable target lesions
Stable disease	**SD**	Between 30% decrease and 20% increase
Progressive disease	**PD**	An increase of > 20% in the sum of the diameters of viable target lesions

Table 12: mRECIST assessment of overall response

Target lesions	**Nontarget lesions**	**New lesions**	**Overall response**
CR	CR	No	CR
CR	Incomplete R / SD	No	PR
PR	No Progress	No	PR
SD	No Progress	No	SD
PD	Any	Any	PD
Any	PD	Any	PD
Any	Any	Yes	PD

5.3 Histopathology of HCC

All available sections of FFPE-HCC tumors were re-evaluated under the guidance of an experienced Pathologist specialized in Hepatopathology (C.L.) according to international standards (WHO 2010). Tumors were classified according to architectural and cytological features into classical HCCs (NOS, or other type). In addition, the presence of tumor cell ballooning, fatty change and cytoplasmic inclusions, giant cell formation, clear cell change as well as intratumoral inflammation, necrosis and fibrosis was recorded.

5.4 Evaluation of c-MET expression

5.4.1 Immunohistochemistry

For detection and semiquantative assessment of cytoplasmic expression of c-MET, IHC was applied. IHC uses the specificity and affinity of immunological antibody-antigen reactions for the detection of epitopes of certain antigens in tissue samples. The development of IHC has been a major contribution to more accurate diagnoses and research. IHC consists of 2 major steps: First, the primary antibody (AB) is applied and binds to its epitope of the antigen in the tissue. There are two major types of primary antibodies: Monoclonal AB are produced in cell culture and show specificity usually only for a single epitope. Polyclonal AB are obtained from serum of animals immunized with the antigen and are directed against different epitopes of the antigen. Second, the signals, which are a specific reaction between antibody and its epitope, are detected. This can be achieved in two ways: In the direct method, the primary AB itself is marked and can be detected. In the indirect method, a secondary AB is applied and binds to the primary AB. The binding of the secondary AB activates a chromogenic, fluorogenic or chemiluminescent reaction with a substrate, depending on the type of detection system used. In standard diagnostic and scientific applications, the indirect method of IHC is commonly used because the signal can be amplified by the secondary antibodies as several molecules of secondary AB can bind to one primary AB.

5.4.2 C-MET IHC using FFPE material

First, tissue samples undergo fixation to stabilize tissue architecture, terminate all biological processes such as activity of proteolytic enzymes and to protect tissue against influences of further processing and staining. Different fixation methods are in use depending on type of tissue and staining method. The most commonly used fixative is formaldehyde that stabilizes proteins by formation of crosslinks between molecules.[64] The formulation used for fixation of tissue for c-MET IHC and in-situ hybridisation (ISH) was 10% neutral buffered formaldehyde (NBF), which is a solution of 4% formaldehyde in phosphate buffer, a formula used for most specimens in histopathological laboratories. After fixation, tissue samples are embedded in paraffin to provide a matrix for sectioning. Due to the nature of paraffin as a hydrophobic substance, all hydrophilic contents of the fixated tissue have to be removed using ethanol and finally xylene as a clearing agent to remove the ethanol before liquid paraffin replaces the xylene. The result of this procedure is a FFPE tissue sample. FFPE blocks are trimmed and sections of 4µm are placed on Superfrost (Fisher Scientific, Waltham, USA) slides.

In our study, we used the CONFIRM anti-Total c-MET (SP44) Rabbit Monoclonal Primary Antibody (Ventana, Tucson, USA). IHC procedure was performed using a Ventana Benchmark autostainer according to manufacturer´s recommendations. Slides were incubated with primary antibody for 16 minutes at 37°C. Signals were produced with 3,3'-Diaminobenzidin (DAB). Slides were counterstained with haematoxylin before mounting.

5.4.3 C-MET IHC semiquantitative score

Results of c-MET IHC were assessed using standard bright field microscopy at a magnification of 400X. Positive signal is a brown membrane-bound staining. A semi-quantitative score from 0 to 3+ was used to quantify c-MET expression in the HCCs. Percentage of tumor cells showing score membrane staining of 1+ to 3+ was recorded to categorize samples as MET-low or MET-high.[65] The mode of immunohistochemical evaluation and semiquantitative scoring is described in Tables 13 and 14.

Table 13: Semiquantitative evaluation of c-MET expression in HCC

Score	Description of staining pattern
0	No membrane staining. The cytoplasm and membrane of the malignant hepatocytes is completely devoid of staining.
1+	Weak membrane staining. The stain may not encircle the entire cell border.
2+	Moderate membrane staining. The stain should involve the complete or nearly complete cell membrane of the tumor cells.
3+	Strong membrane staining. The stain should show complete encirclement of the cells.

Table 14: Definition of c-MET status by IHC

c-MET status	Frequency of scores
MET-low	≤ 50% of HCC cells with c-MET score ≥ 2+
MET-high	≥ 50% of HCC cells with c-MET score ≥ 2+

5.4.4 mRNA in situ hybridisation

In situ hybridization (ISH) uses a labelled nucleic acid probe to localize a specific sequence of deoxyribonucleic acid (DNA) or ribonucleic acid (RNA) in cells. The principle of the method is the specific covalent binding between the nucleobases guanine + cytosine and adenine + thymine (uracil in mRNA) that facilitates the hybridisation of the labelled nucleic acid sequence of the probe to its complementary target DNA or RNA in the tissue, cell or metaphase chromosome. Hence, the labelled probe can be detected by a chromogenic or flourogenic reaction (FISH).[66] The main difference between IHC and ISH is the target of the labelled probe: IHC works on the protein level while ISH is used to localize certain sequences of RNA and DNA. The level of mRNA normally correlates with the level of gene expression in cells. ISH is a useful research tool in particular in neoplastic diseases, where an altered expression pattern of oncogenes and tumor suppressor genes is crucial for understanding carcinogenesis and resistance to therapy.

In our study, we used the RNA Scope 2.0 Red (Advanced Cell Diagnostics, Hayward, USA) system to assess c-MET expression on the mRNA level. RNA Scope is a novel in situ ISH assay that helps to localize and quantify mRNA in intact cells in tissue sections. Compared to other ISH methods, RNA Scope features a particularly low signal to noise-ratio ("background") due to a special target probe design. Target-specific signals are amplified while background noise from nonspecific hybridisations is suppressed. A series of probes hybridizes to the target RNA. Each probe contains a 25-base sequence of RNA that is complementary to the target RNA. Signals are generated by two probes hybridising next to each other. Then the Z-shaped probes connect together with the preamplifier. This preamplifier connects to the amplifier and eventually to the labelled probe which is connected to an alkaline phosphatase molecule or horseradish peroxidase (HRP) for chromogenic reaction with Fast Red or 3,3´-diaminobezidine (DAB). Due to the presence of bile which can have a brownish colour in some types of HCC, we chose Fast Red as a chromogenic substrate.[67]

5.4.5 C-MET mRNA in situ hybridisation

ISH was performed according to manufacturer's protocol. Briefly, FFPE HCC tissue was cut to sections of 5 µm thickness. Sections were mounted on Superfrost slides (Fisher Scientific) and were processed as recommended by the manufacterer. Slides were baked in a dry oven at 60°C. Then, slides were placed on a TissueTek slide rack (Sakura, Alphen, Netherlands) and submerged in Xylene (2x 5min) and 100% Ethanol (2x 1min) for deparaffinization. Thereafter, sections were air-dried at room temperature (RT). Next step was incubation with hydrogen peroxide solution (Pretreat 1) for 10min at RT followed by incubation in citric acid buffered lithium dodecyl sulfate (Pretreat 2) at boiling temperature of 100-103°C on a hot plate for 15min. Then the slides were rinsed with de-ionised water. Protease digestion was performed with 10µg/ml protease in propane-1,2-diol solution (Pretreat 3) for 30min at 40°C with slides incubated in a HybEZ hybridisation oven (Advanced Cell Diagnostics). Target probes for c-MET, positive control and negative control were applied for 2 hours at 40°C using consecutive sections of HCC tissue. Thereafter, slides were incubated in the hybridisation oven. According to manufacturer's protocol, preamplifier, ready-to-use preamplifier, signal enhancer and amplifier

followed by the label probe were applied for their specific time in the hybridisation oven or at room temperature. The workflow is illustrated in Table 15. The exact formulation of reagents used for signal amplification has not been released by the manufacturer. Between each of the steps, slides were incubated in washing buffer (0.03% lithium dodecyl sulphate) for 2x2min at RT. Chromogenic detection was performed with Fast Red followed by counterstaining with haematoxylin and eosin (HE).

Table 15: C-MET RNA Scope workflow

Hybridisation step	**Incubation time**	**Incubation temperature**
AMP 1	30 min	40°C
AMP 2	15 min	40°C
AMP 3	30 min	40°C
AMP 4	15 min	40°C
AMP 5	30 min	RT
AMP 6	15 min	RT

5.4.6 C-MET RNA Scope positive and negative controls

For the RNA Scope assay, positive and negative controls were included for every assay of a FFPE tissue sample to control for specificity and sensitivity. As positive control for general mRNA expression, the mRNA of a gene encoding the house keeping enzyme Peptidyl-prolyl cis-trans isomerase (PPIB) was used. PPIB is ubiquitously expressed in various types of human tissue and in liver.[68] If the ISH of PPIB revealed positive signals, we considered the quality of RNA in the FFPE sample of the tumor sample sufficient for further analysis. If the positive control failed, while the positive control of another sample in the same run of the assay was sufficient, the positive control hybridisation was repeated. If the result was negative, this sample was excluded from further analysis. A FFPE sample of a HCC with satisfying quality of RNA was used as an external positive and negative control in each experiment. The probe for the negative control was targeted to 3,3'-Diaminobenzidin (dapB), a bacterial gene which is not expressed in eukaryotic cells.

5.4.7 C-MET RNA Scope semiquantitative score

We assessed the results of the c-MET RNA Scope according to the recommendations given by the manufacturer. These specifications are illustrated in Table 16. Key point is the number of signals present within the boundaries of each cell (cell membrane). A signal is represented by punctate red dots visible in standard bright field microscopy at a magnification of at least 200X. Each spot represents one copy of mRNA of the c-MET gene in the cytoplasm. In case of high expression, single signal spots may overlap and form spot clusters. For semiquantative evaluation of c-MET on the RNA level the scoring system provided by the manufacturer was used. Evaluation was performed using standard bright field microscopy at a magnification of 200 and 400X.

Table 16: Semiquantitative score for c-MET RNA Scope

Staining score	**Microscope objective scoring**
0	No staining or <1 dot to every 10 cells
1	1-3 dots/cell.
2	4-10 dots/cell. Very few clusters.
3	>10 dots/cell. Less than 10% of positive cells have dot clusters.
4	>10 dots/cell. More than 10% of positive cells have dot clusters.

5.4.8 C-MET RNA Scope quantitative score

For quantitative image analysis we used RNA Scope Spot Studio software (Definiens, Munich, Germany). This software is does not require specific training in digital image analysis techniques and is easy to apply. Focus stacked images were first prepared to enable Spot Studio analysis technique. Images were captured with a Zeiss Observer-Z1 inverted microscope (Zeiss, Oberkochen, Germany). Multiple tiles (3x3) were captured at 40X with 10 focus-stacks using the MosaiX module of the AxioVision software (Zeiss). Each stitched image corresponds to an area of approximately 3981x2980 pixels (0.62 x 0.45 mm). Images were saved as .jpg files. Spot Studio also supports various other file formats such as .zvi, .lif or png.

The workflow of Spot Studio comprises several steps which are described in Figure 15 First, images are loaded, regions of interest (ROI) and several morphological parameters such as type of stain, nucleus diameter, intensity of spot stain, spot

diameter have to be defined. Spot Studio allows the user to obtain statistical data of cell count/region of interest and the number of spots per cell. The number of spots per cell is also displayed in a histogram. Inadequate settings directly influence cell count and signal/cell rate.

Figure 6: Threshold settings panel

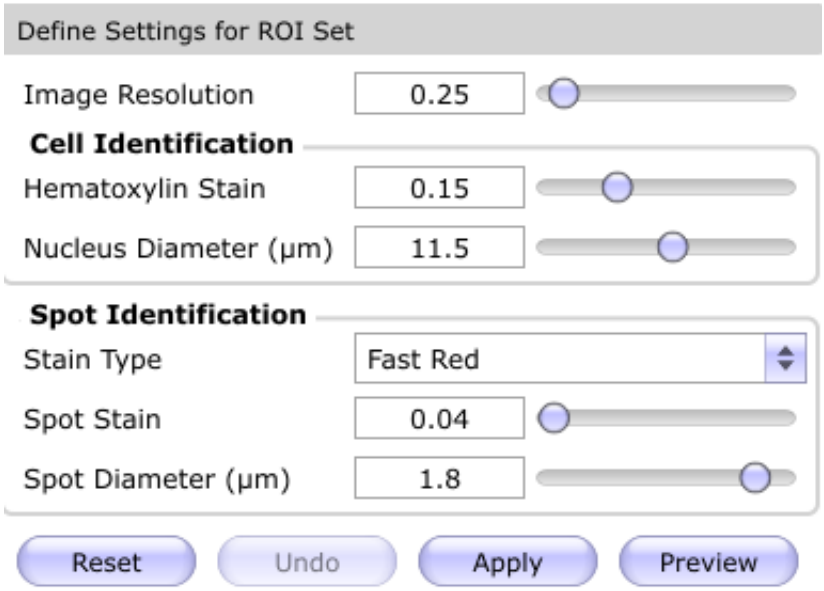

Figure 6: The threshold setting panel includes several cell and spot/signal identification parameters. Screenshot RNA Scope Spot Studio.

Figure 7 and 8 illustrate the cell identification process with screenshots of RNA Scope. The cell identification parameters define the cell count and thereby influence the number of spots per cell. Cell identification parameters are hematoxylin level and nucleus diameter. In addition the size of cells is influenced by the nucleus diameter. The cell identifaction parameters determine the number of cells counted and therby influence the value of signals per cell. These parameters have to be set manually using a sector (region of interest) of each slide. If parameters are set adequately, each cell is encircled by a green line.

Figure 7: HE level settings

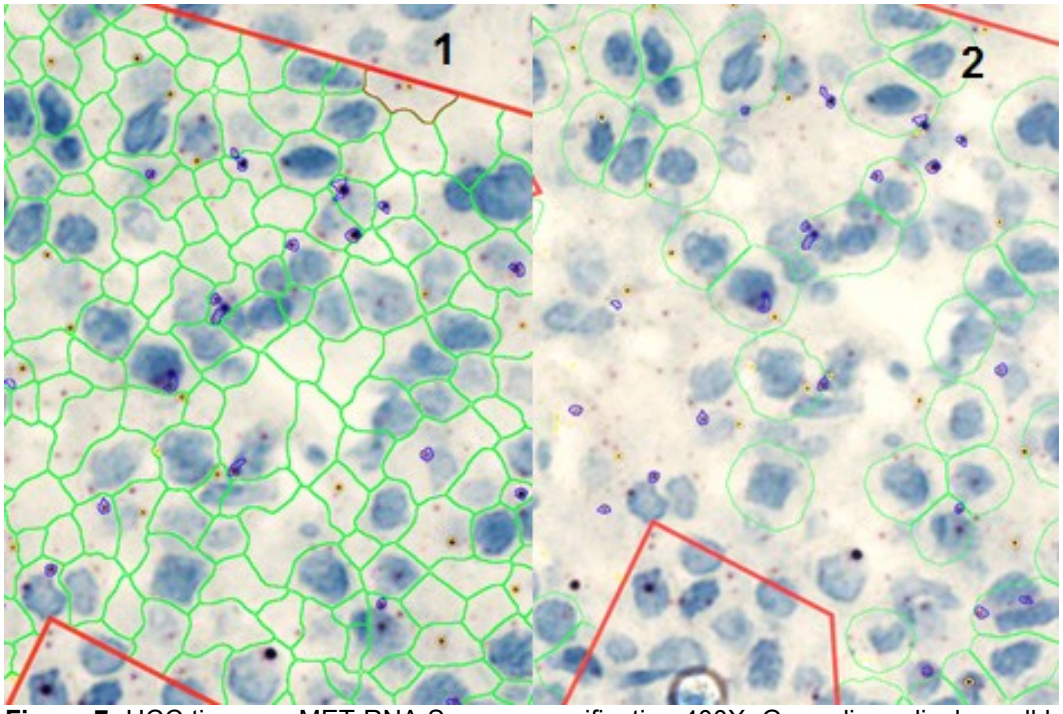

Figure 7: HCC tissue, c-MET RNA Scope, magnification 400X. Green lines display cell bounderies identified by automated image analysis. 1: HE level setting inadequately low resulting in too high number of cells counted. 2: HE level setting inadequately high, resulting in too few cells counted. Screenshot of RNA Scope Spot Studio.

Figure 8: Nucleus diameter settings

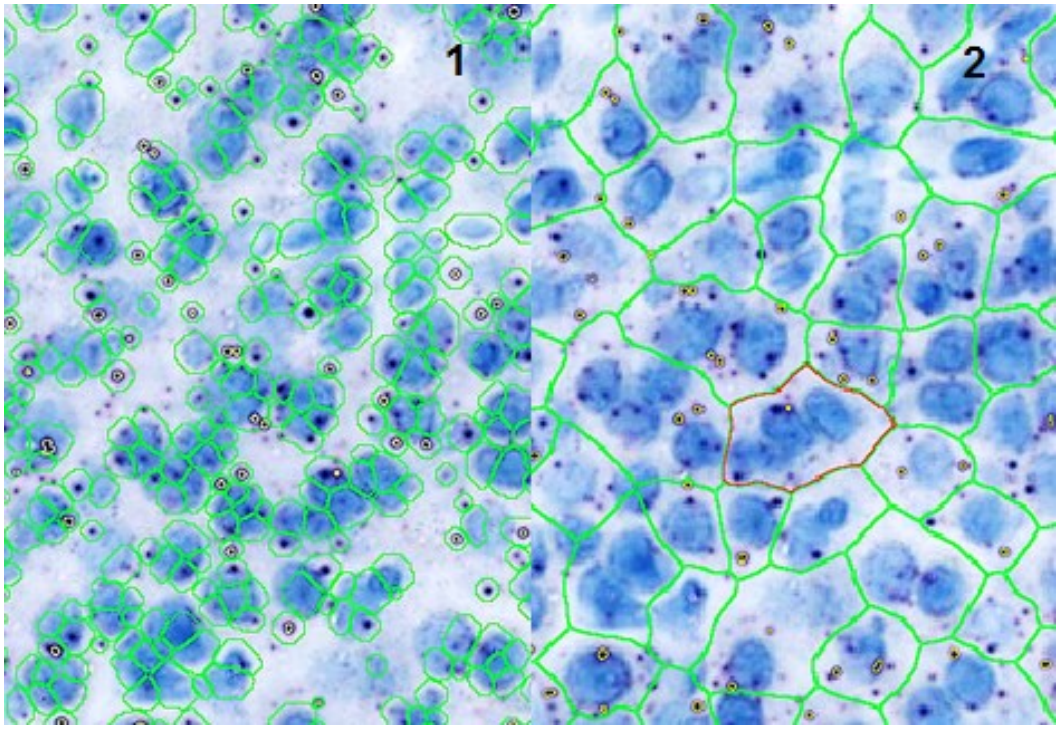

Figure 8: HCC tissue, c-MET RNA Scope, magnification 400X. Green lines display cell bounderies identified by automated image analysis. 1: nucleus diameter setting inadequately low resulting in too high number of cells counted. 2: nucleus diameter setting inadequately high, resulting in too few cells counted. Screenshot of RNA Scope Spot Studio.

The spot identification parameters determine sensitivity and specificity of signals counted. In an ideal setting (see Figure 11), each signal, which accounts for a RNA copy, is marked by a yellow dot while there are no yellow dots in areas showing solely background noise. Spot clusters, which are defined as signals generated by overlying single spots. These clusters are encircled by a blue line. Figure 9 and 10 display screenshots of the signal identification process. RNA Scope Spot Studio uses the number and size of spot clusters the calculate the value of spots estmated.

Figure 9: left: Spot stain settings

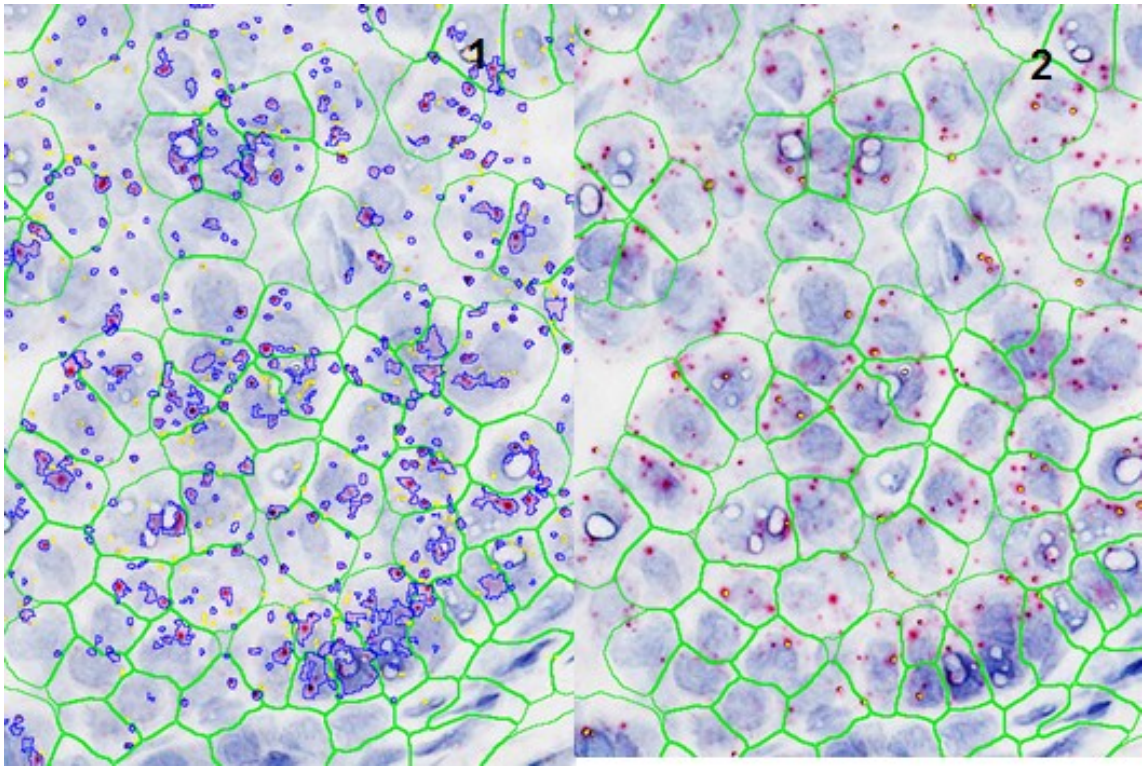

Figure 9: HCC tissue, c-MET RNA Scope, magnification 400X. Yellow signals show single spots, while blue signals show spot clusters as recognised by automated image analysis.. Red, punctate dots are amplified and detected copies of c-MET mRNA. 1: Spot stain settings inadequately low resulting in high rate of false-positive signals and too high cluster:single spot ratio. 2: Spot stain settings inadequately high resulting in a high rate of false-negative signals, which corresponds to a high number of red dots without yellow accentuation. Screenshot RNA Scope Spot Studio.

Figure 10: Spot diameter settings

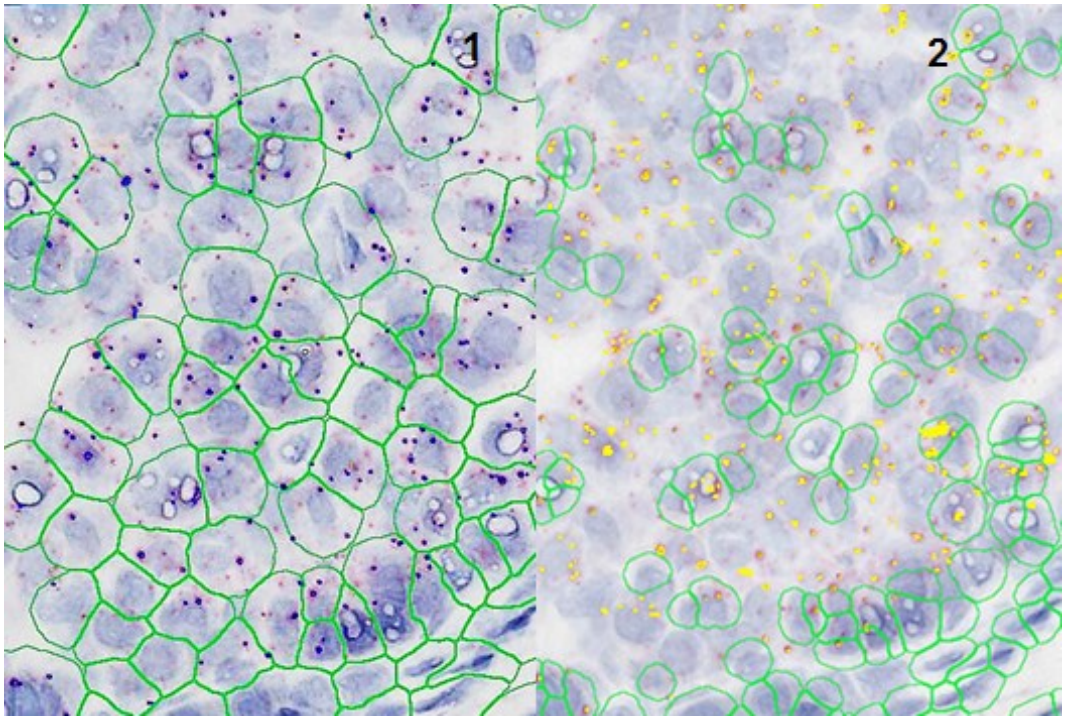

Figure 10: HCC tissue, c-MET RNA Scope, magnification 400X. Yellow signals illustrate single spots, while blue signals stand for spot clusters as recognised by automated image analysis. 1: Spot diameter settings inadequately high resulting in a high rate false-negative signals. 2: Spot diameter settings inadequately low, resulting in a high rate of false-positive signals appearing as yellow lines. Screenshot RNA Scope Spot Studio.

Figure 11: Optimal settings of RNA Scope Spot Studio

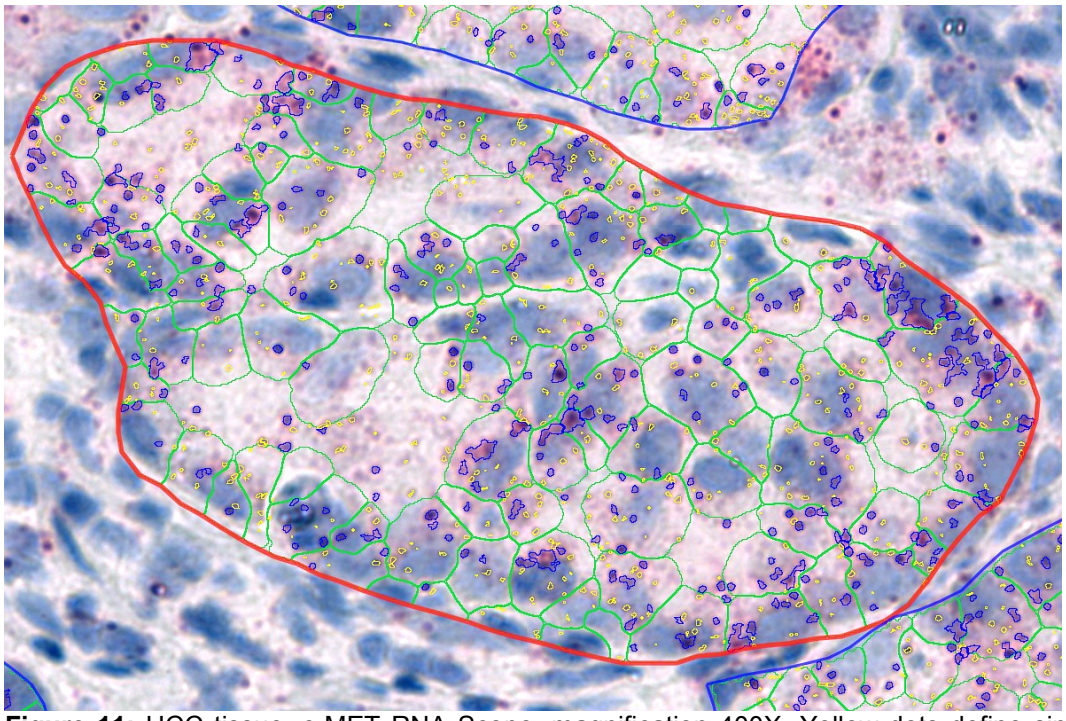

Figure 11: HCC tissue, c-MET RNA Scope, magnification 400X. Yellow dots define single spots while blue lines encircle spot clusters, each cell boundery is encircled by a green line, the red frame specifies the region of interest. Screenshot RNA Scope Spot Studio.

RNA Scope Spot Studio provides both single spot and spots estimated values, the latter containing estimated number of signals deriving from spot clusters. Histograms show if there is an overweight of signals with a very high intensity of signals contributing to the estimated spot count. If this is the case, the single spot count may be considered to have higher specificity than the number of spots estimated. Figure 12 is sample screenshot of the analysis of a case with an overweight of false-positive spot clusters.

Results of RNA Scope Spot Studio can be exported as a .xls file, histograms showing the distribution of spots per cell are calculated automatically and can be exported as a .png or .jpg file.

Figure 12: Histograms generated with RNA Scope Spot Studio

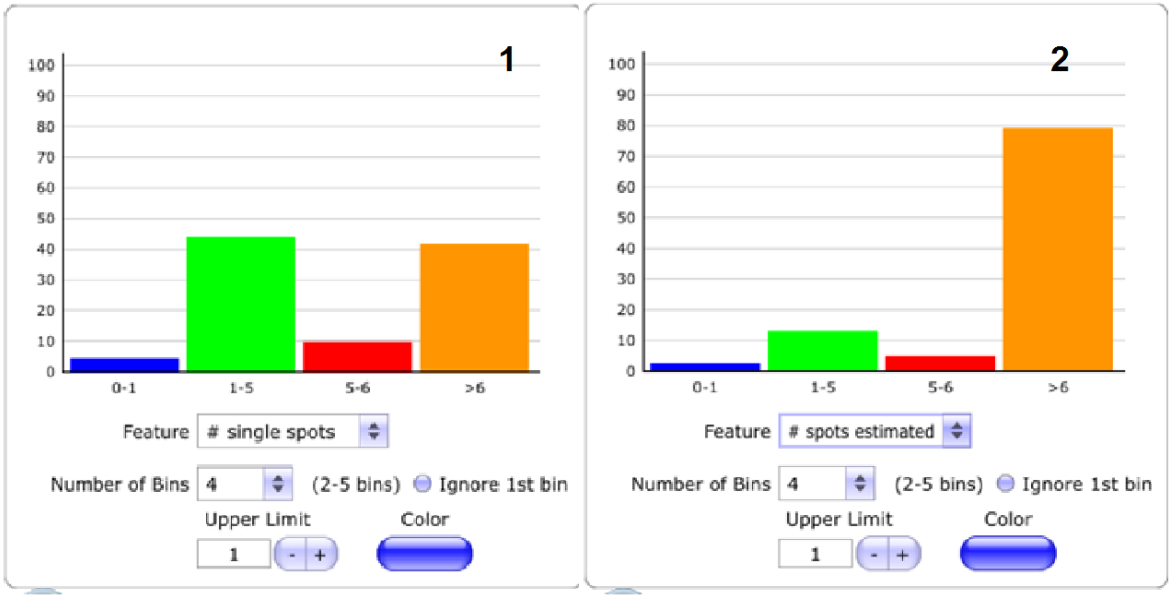

Figure 12: The blue, green, red and orange bars stand for the share of single spots (1) and spots estimated (2) deriving from cells with 0-1, 1-5, 5-6 and >6 signals per cell. In the case of (1), there is an equal distribution while in the case of (2), the overwhelming majority of signals derive from cells with >6 signals, which indicates the possibility of false-positive spot clusters. In this case, the number of single spots may have a higher specificity than the number of spots estimated. Screenshot RNA Scope Spot Studio.

6 Results

6.1 Patient cohorts

19 patients, who fulfilled the inclusion criteria were stratified in response groups according to the m-RECIST scheme. 8 patients were considered to respond to sorafenib (stable disease) while 11 were classified as non-responders to therapy (progressive disease).

To control confounding, data about clinical, biochemical and histopathological parameters was collected and analysed using appropriate statistical tests. Clinical and biochemical characteristics of responders and non-responders to sorafenib are detailed in Table 16, histopathologic features are summarised in Table 17. Age and sex of our study cohorts matched with epidemiological data reported in literature (median age approximately 60a ± 12a, male>female patients). As expected, biochemical parameters indicating liver damage such as AST, ALT and GGT were increased in some patients. This may be explained by the fact that HCC is the final stage of liver diseases (AFLD, NAFLD, viral hepatitis). Aetiology and stage of cirrhosis are distributed equally between patients with response and non-response to sorafenib. Of all clinical and biochemical features analysed, only AFP showed moderate correlation with non-response (Pearson´s correlation coefficient r=0.38; significance level of p=0.013). Because of the variance of AFP values, we also calculated a t-test using ln(AFP), which confirmed the findings (r=0.59 / p=0.008). Previous research showed that higher AFP levels correlate with advanced tumor stage with the highest levels detected in patients with metastatic tumors, which is consistent with the significant correlation of AFP and sorafenib resistance in this study.[69]

The majority of the FFPE material used in our study in both response groups originated from biopsies, only a minor share from liver resection or autopsy. Analysis of the data summarised in Table 17 did not reveal any significant relation between histopathological features and response class with significance level always lower the cut-off value of p=0,05. According to this, the histopathological features evaluated in this study appear to be equally distributed between HCC patients with response and resistance to sorafenib. All HCCs showed architectural features of the

classical HCC type. Among patients with SD and PD, most common architectural patterns were trabecular and combined trabecular-pseudoglandular pattern. According to this, the majority of tumors had an intermediate histological grade of differentiation (G2). Features such as bile production and clear cell change were rare in HCCs of both response groups.

Table 16: Clinical and biochemical features of HCC patients as defined by response to sorafenib

	Responders n / %	**Non-responders n / %**	**Significance ***
Age mean / median / SD	53-84 62.38 / 61 / ±10.18	44-76 61.91 / 65 / ±12.14	p=0.93
Sex male female	 7 / 87.5% 1 / 12.5%	 9 / 81.82% 2 / 18.18%	p=0.44
AST (U/l) mean / median / SD	19-77 48.75 / 52.5 / ±22.51	32-193 100 / 81 / ±54.3	p=0.23
ALT (U/l) mean / median / SD	15-133 55 / 47 / ±42.36	17-120 41.63 / 33 / ±28.69	p=0.42
GGT (U/l) mean / median / SD	42-721 297.75 / 190 / ±279.6	27-1483 342.55 / 198 / ±430.54	p=0.81
AP (U/l) mean / median / SD	74-460 176.5 / 127 / ±127.16	89-708 209.46 / 144 / ±177.23	p=0.66
Thrombocytes G/l mean / median / SD	96-360 238.25 / 242 / ±103.32	76-536 219.45 / 200 / ±118.82	p=0.72
Bilirubin total (mg/dl) mean / median / SD	0.23-1.75 0.67 / 0.56 / ±0.48	0.41-2.98 1.07 / 0.81 / ±0.78	p=0,22
Kreatinin (mg/dl) mean, median, SD	0.82-1.25 0.88 / 0.84 / ±0.19	0.65-1.22 0,89 / 0.91 / ±0.18	p=0.88
INR within normal range (0.8-1.2)	100%	100%	

MELD score (6-40 pts) mean / median / SD	6-12 8.25 / 8 / ±1.83	6-13 8.55 / 8 / ±2.02	p=0.75
Serum albumin (mg/dl) mean / median / SD	3-4.4 3.75 / 3.85 / ±0.59	3.2-4.5 3.86 / 4 / ±0.35	p=0.60
AFP mean / median / SD	1.8 - 225.4 35.85 / 7.3 / ±76.95	4-48994.5 10095.03 / 843 / ±16888	p=0.013 r=0.38
Aetiology of liver disease Non-viral: ASH, NASH Thereof: ASH Thereof: NASH viral hepatitis:	 6 / 75% 5 / 62.5% 1 / 12.5% 2 / 25%	 6 / 54.55% 4 / 36.36% 2 / 18.18% 5 / 45.45%	p=0.36
Cirrhosis – CPS (n, %) no evidence for cirrhosis 5-6 pts (A) 7-9 pts (B)	 1 / 12.5% 5 / 62.5% 2 / 25%	 1 / 9.09% 8 / 72.73% 2 / 18.18%	p=0.89

* Statistical analysis with t-test for independent variables or contingency tables and Chi²-test.

Table 17: Histopathological features of HCC patients as defined by response to sorafenib

	Responders n / %	**Non-responders n / %**	**Significance***
Origin of tissue			
biopsy	7 / 87.5%	7 / 63.63%	p=0.46
resectate	1 / 12.5%	3 / 27.27%	
autopsy	0	1 / 9.09%	
Anatomical site			
primary tumor	8 / 100%	9 / 81.82%	p=0.2
liver metastasis of HCC		2 / 18.18%	
Histologic type			
HCC NOS	8 / 100%	11 / 100%	
fibrolamellar HCC	0	0	

Histologic grade			
G1	0	2 / 18.18%	p=0.35
G2	5 / 62.5%	7 / 63.63%	
G3	3 / 37.5%	2 / 18.18%	
Architectural pattern			
solid	1 / 12.5%	2 / 18.18%	p=0.46
trabecular	3 / 37.5%	2 / 18.18%	
pseudoglandular	0	0	
combined trabecular – pseudoglandular	2 / 25%	3 / 27.27%	
combined trabecular – solid	1 / 12.5%	4 / 36.36%	
combined trabecular fibrolamellar	1 / 12.5%		
Inflammation in tumor			
present	2 / 25%	0	p=0.08
absent	6 / 75%	11 / 100%	
giant cell formation			
present	0	1 / 9.09%	p=0.38
absent	8 / 100%	10 / 90.91%	
tumor steatosis			
present	3 / 37.5%	1 / 9.09%	p=0.13
absent	5 / 62.5%	10 / 90.91%	
clear cell component			
present	0	1 / 9.09%	p=0.38
absent	8 / 100%	10 / 90.91%	
bile production			
present	1 / 12.5%	1 / 9.09%	p=0.81
absent	7 / 87.5%	10 / 90.91%	
tumor necrosis			
present	0	3 / 27.27%	p=0.11
absent	8 / 100%	8 / 72.73%	
inclusion bodies			
absent	7 / 87.5%	11 / 100%	p=0.23
MDBs + IHBs	1 / 12.5%	0	

* Statistical analysis with contingency tables and Chi²-test.

6.2 C-MET expression in HCC tissue by IHC and RNA Scope

Results of c-MET of HCC with c-MET protein expression scores 0-3 tissue are illustrated in Figure 13.

Figure 13: Results of c-MET IHC

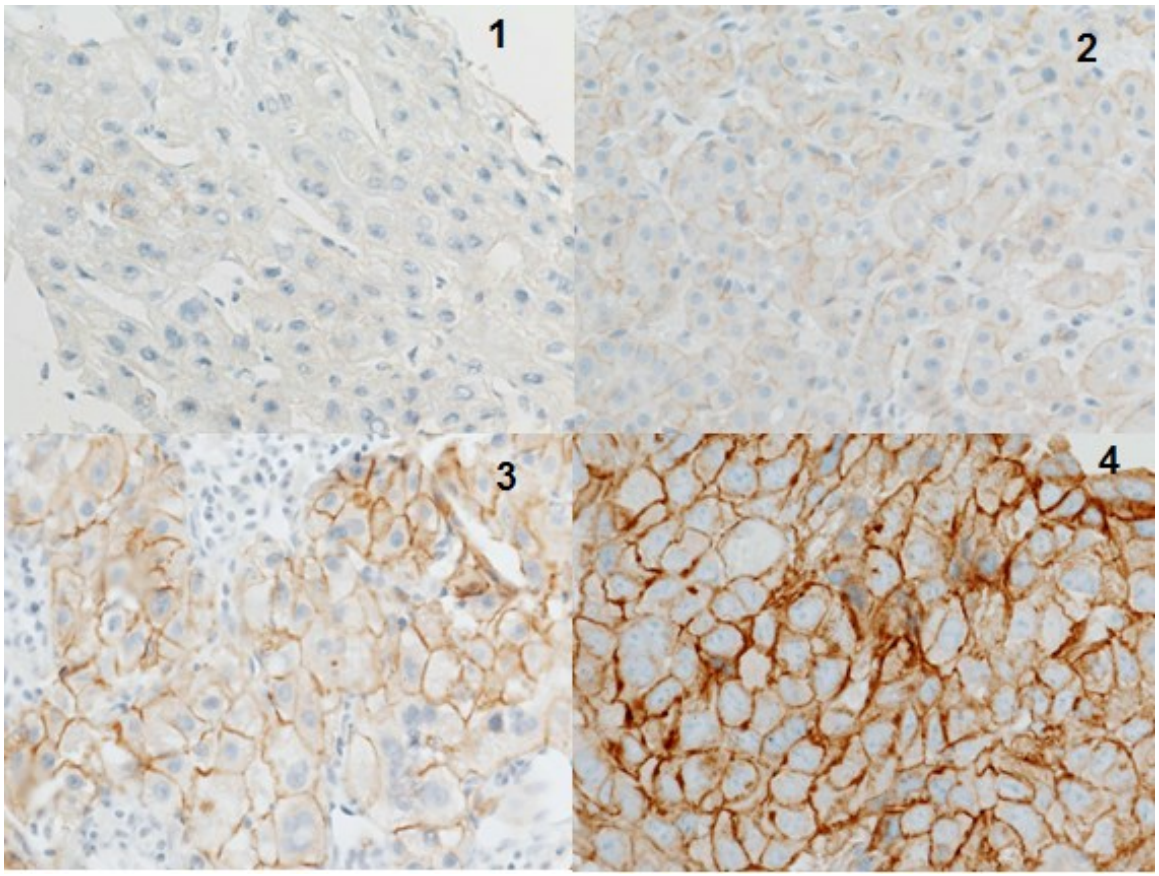

Figure 13: HCC tissue, c-MET IHC, magnification 400X. Positive signal is a brown, cytomembranous stain. 1: IHC score 0: No membrane staining. The cytoplasm and membrane of the malignant hepatocytes is completely devoid of staining. 2: IHC score 1: Incomplete membrane staining. The stain does not encircle the entire cell border. 3: IHC score 2: Moderate membrane staining. Cells show near or complete encirclement of the stained cell. 4: IHC score 3: Strong membrane staining. This score shows complete encirclement of the cells.

Figure 14 displays results of RNA Scope and illustrates the score we used for semiquantitative evaluation of c-MET mRNA expression.

Figure 14: Results of c-MET RNA Scope

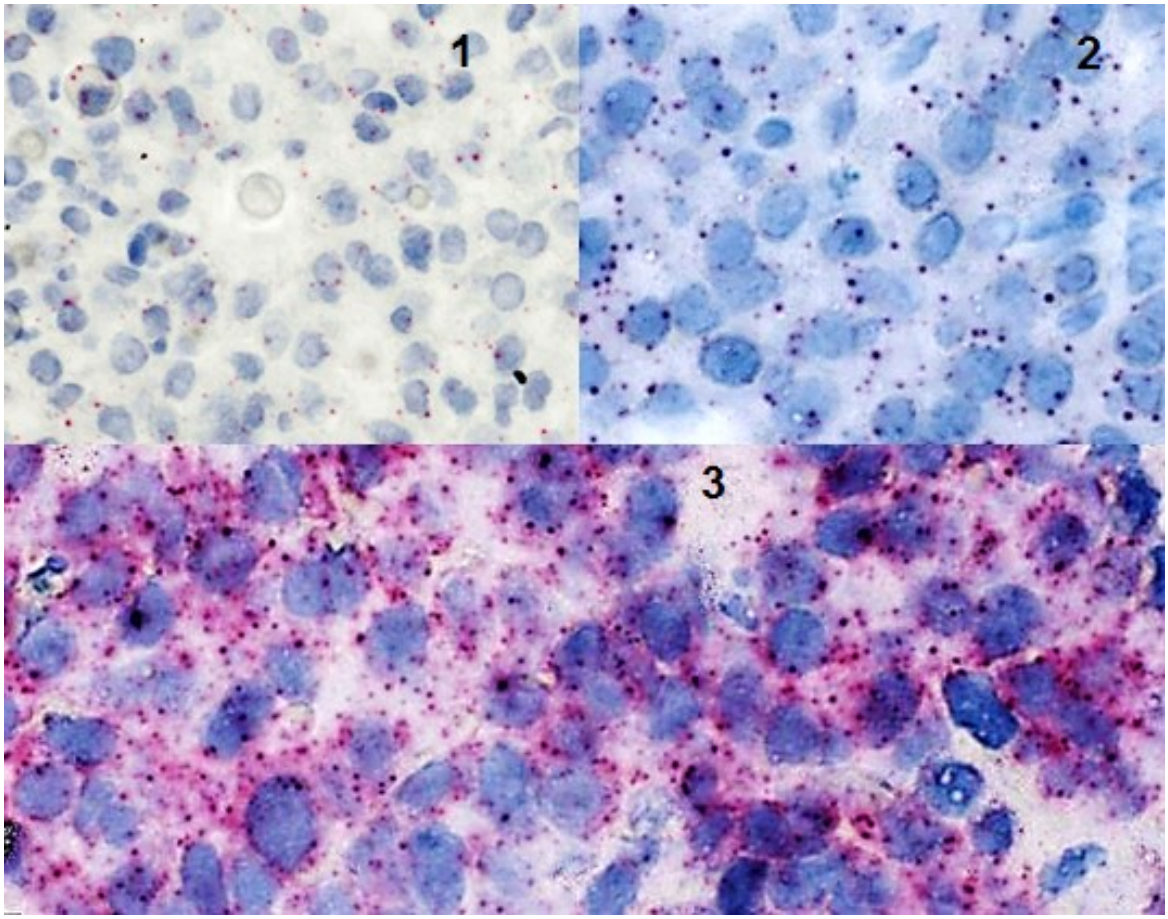

Figure 14: HCC tissue, c-MET RNA Scope. Red, circulate dots and dot clusters account for signals. 1: RNA Scope score 1: 1-3 dots/cell. 2: RNA Scope score 2: 4-10 dots/cell. Very few clusters. 3: RNA Scope score 3: >10 dots/cell. Less than 10% of positive cells have dot clusters.

We also evaluated the expression of c-MET RNA in bile ducts in non-neoplastic liver tissue (Figure 15). However, utility of this internal positive control was limited by the non-availability of non-neoplastic liver tissue in some samples. While tissue samples from liver resections were selected to combined portions of HCC and non-neoplastic tissue, tissue samples obtained by biopsy often lacked non-neoplastic tissue. Examples of positive and negative control slides of RNA Scope are shown in figure 16.

Figure 15: C-MET expression in bile ducts

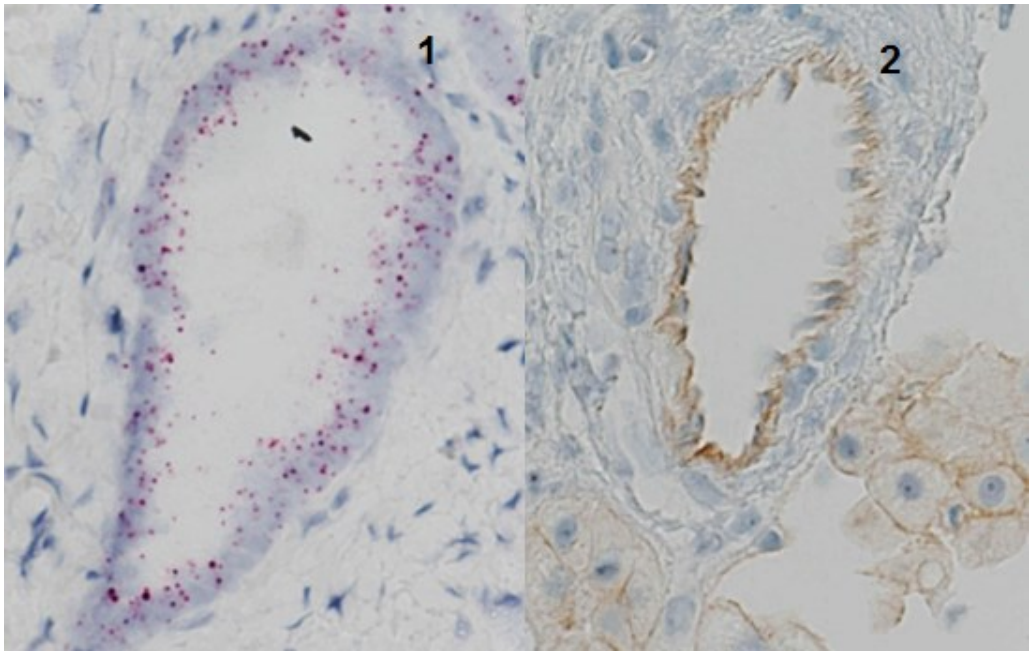

Figure 15: Non-neoplastic liver tissue, magnification 400X. 1: C-MET RNA Scope. Red punctate dots represent signals deriving from c-MET mRNA in cholangiocytes. 2: C-MET IHC: Brown, cytomembranous stain shows c-MET protein expression in bile ducts.

Figure 16: Positive and negative control of RNA Scope

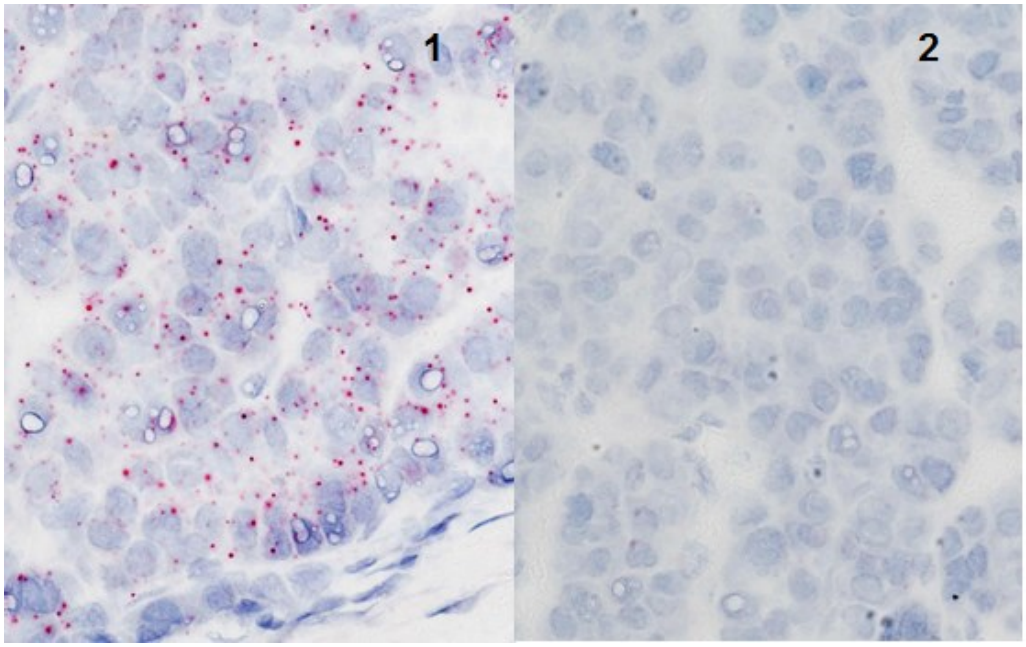

Figure 16: HCC tissue, magnification 400X.1: PPIB RNA Scope, this positive control shows a satisfying result, score 3. 2: DapB RNA Scope, this negative control does not show and false-positive signals.

Results of c-MET expression by IHC and RNA Scope are illustrated in Table 18, Table 19 displays results of c-MET IHC and ISH for each patient of the study.
A t-test verified correlation between the results of IHC and RNA Scope: Pearson´s correlation coefficient was r=0.51 (p=0.026) for ISH (spots estimated) and r=0.558 (p=0.013) for ISH (single spots). There was no correlation found between response to sorafenib and c-MET expression by IHC and RNA Scope (p=0.6 for c-MET IHC and p=0.24-0.57 for c-MET RNA Scope semiquantitative score and quantitative score using single spots ans spots estimated values).

Table 18: c-MET expression of HCC patients as defined by response to sorafenib

	Responders n / %	**Non-responders n / %**	**Significance***
c-MET IHC semiquant. score			
high	2 / 25%	4 / 36.36%	p=0.6
low	6 / 75%	7 / 63.64%	
c-MET RNA Scope semiquant. Score			
RNA quality insufficient	2 / 25%	2 / 18.18%	p=0.27
Staining score 0	1 / 12.5%	2 / 18.18%	
Staining score 1	3 / 37,5%	6 / 75%	
Staining score 2	2 / 25%	0	
Staining score 3	1 / 12.5%	1 / 9.09%	
c-MET RNA Scope quant. image analysis spots estimated	0.03-12.53	0.07-4.7	p=0.24
mean / median / SD	3.05 / 1.32 / 4.73	1 / 0.55 / 1.43	
c-MET RNA Scope quant. image analysis single spots	0.03 – 1.3	0.06 – 2.19	p=0.57
mean, median, SD	0.74 / 0.77 / 0.51	0.56 / 0.39 / 0.63	

* Statistical analysis with t-test for independent variables or contingency tables and Chi²-test.

Table 19: Response group and c-MET expression evaluated by IHC and ISH

patient number	response group	c-MET IHC	c-MET RNA Scope semiquant.	c-MET RNA Scope spots estimated	c-MET RNA Scope single spots
1	PD	high	1	1.23	0.54
4	PD	low	1	0.52	0.39
2	SD	low	0*	0*	0*
3	SD	low	0*	0*	0*
5	SD	high	2	12.53	0.73
6	SD	low	0	0.03	0.03
11	SD	high	2	1.58	1.3
13	SD	low	1	0.52	0.33
16	SD	low	1	2.57	1.28
18	SD	low	1	1.06	0.8
7	PD	low	0*	0*	0*
8	PD	high	1	0.75	0.43
9	PD	low	0*	0*	0*
10	PD	low	0	0.07	0.06
12	PD	low	1	0.24	0.23
14	PD	low	0	0.27	0.27
15	PD	high	1	0.64	0.55
17	PD	high	3	4.7	2.19
19	PD	low	1	0.55	0.39

(* = RNA quality insufficient for analysis)

6.3 Characteristics of IHC and RNA Scope

In Table 20, the knowledge about the workflow and economic resources of well-established IHC and novel RNA Scope that was obtained in this study is summarised.

Table 20: Characteristics of IHC and RNA Scope

	IHC	**RNA Scope**
Target	C-MET protein	C-MET mRNA
Application status	In use for routine diagnostics and research	Research, evaluation of method
Automatisation	Automated platform used in this study	Manual platform used in this study, automated platform is available
Cases excluded for tissue quality	0/19	4/19
Time consumption of assay	4h for 30 tumor cases	10h for 6-8 tumor cases
Scoring system	Semiquantitative	Semiquantitative and quantitative by automated image analysis (morphometry)
Financial resources / case	20€	150€ (assay), 20€ (image analysis)

6.4 Survival analysis: Kaplan-Meier plots

Kaplan-Meier plots and log-rank tests were used to investigate differences in OS between HCC patients with SD and PD according to m-RECIST, with c-MET expression by IHC low and high and with c-MET expression by RNA Scope (spots estimated and single spots) low and high.

Figure 17: Survival analysis: Kaplan-Meier plots

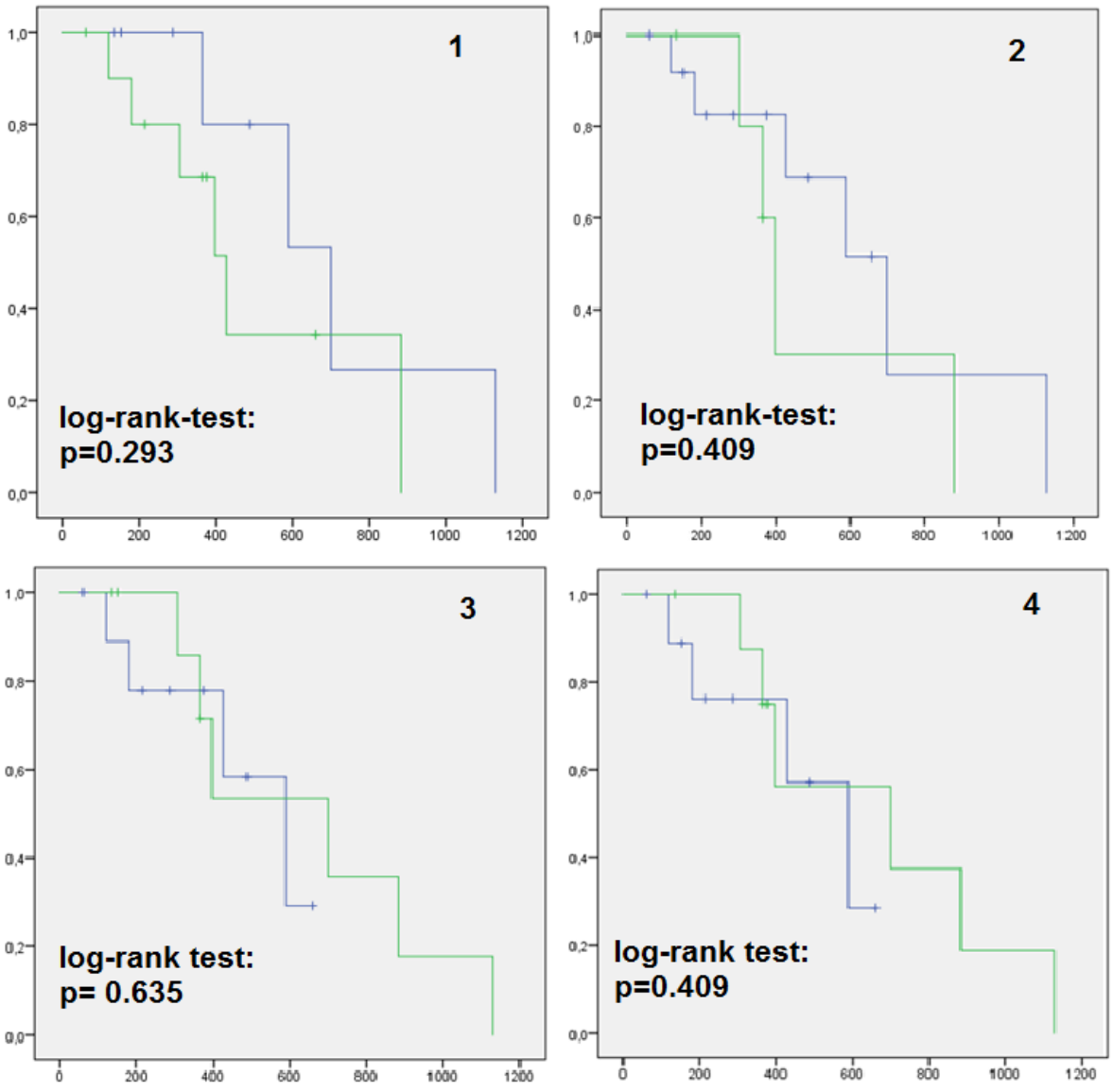

Figure 17: 1: KM plot for HCC patients with SD and PD during treatment with sorafenib according to mRECIST. The result of the log-rank test (>0,05) indicates no significant difference in OS. 2: KM plot for patients with c-MET IHC status low and high. 3: KM plot for patients with c-MET RNA Scope (spots estimated) low and high. The cutoff value between 50% low and high was calculated with 0.55 spots/cell. 4: KM plot for patients with c-MET RNA Scope (single spots) low and high. The cutoff value between 50% low and high was calculated with 0.39 spots/cell. KM plots were calculated with SPSS 23.

7 Discussion

Objective and reproducible measurements are crucial in the evaluation of markers predicting the response and/or prognosis as they are of great influence on patient management. However, observer related bias is inherent to any semiquantitative scoring method for the assessment of morphological features. C-MET expression in HCC tissue assessed by classical standardized semiquantitative scoring of IHC signals obtained by the CONFIRM anti-Total c-MET antibody serves as a predictive marker for the response to tivantinib, a novel potential second-line drug and possibly also to sorafenib, the only drug currently approved for the treatment of advanced stage HCC. This approach is limited by interobserver variation, as indicated by Cohen´s Kappa of only 0.55[70]. Such moderate levels of inter-observer agreement may be improved by the use of a quantitative method for the assessment of c-MET or other protein expression rather than a semiquantitative preocedure. Automated image analysis (morphometry) has the potential to improve consistency and accuracy of the interpretation of morphological features. For instance, in the breast cancer setting, automated image analysis could resolve equivocal scoring of immunohistochemistry of cytoplasmatic receptors (HER2) in tumor tissue.[71]

In our study, we used the novel RNAscope assay to quantitatively analyse c-MET RNA expression in HCC by morphometry. We found this assay user friendly and easy to apply. Our data indicate that there is a good correlation of results of c-MET expression obtained by classical Confirm Anti-Total C-MET IHC and RNA scope. However, as a quantitative method, RNA scope may be a valuable tool to decrease intra- and interobserver bias in particular when used in clinical studies. A factor limiting the applicability of the mRNA scope is RNA quality which proved to be insufficient in 21% of our FFPE-samples. Another potential obstacle for the application in clinical routine is that in comparison to classical IHC techniques mRNA scope is more time consuming. Hands-on time for the RNA scope assay, excluding preparation of FFPE material, is approximately 10 hours for 6-8 tumor samples as compared to 4 hours and as many as 30 samples for the IHC method when an automatic stainer is employed. From an economical point of view, RNA scope is also more expensive. The cost of material for RNAscope is 170 € and 20€ for classical IHC per sample, respectively.

The second aim of this study was to evaluate the utility of c-MET RNA and/or protein expression in HCC as a predictive marker for the response to sorafenib. To assess the relation between response to sorafenib and c-MET expression, patients were classified in response groups according to the m-RECIST criteria. Although previous studies indicated a correlation between sorafenib resistance and c-MET overexpression (c-MET high), in our study no correlation between response class and c-MET expression ($p=0.24$ and $p=0.6$) was found. Furthermore, the length of overall survival of patients with high and low c-MET status did not differ. The exact causes for these discrepancies are not known. However, several factors may be responsible, the most important of which is the low sample number. However, patients with advanced HCC and sorafenib treatment may be difficult to study in sufficient numbers in a single center. In our study from 68 patients that were initially identified as potentially eligible only 19 could be analysed. Most cases were because sorafenib was discontinued due to side effects, death before three months of follow up, insufficient biopsy or lack of follow-up.

In conclusion, the novel RNA Scope assay provides results consistent to those obtained with the well-established semiquantitative IHC method. Quantitative assessment using RNA scope may help to overcome the problems with observer related bias in particular in the setting of clinical studies. This aspect as well as the utility of C-MET expression as predictive and prognostic marker should be investigated in further studies involving larger patient cohorts.

8 References

[1] **Waldeyer, A. and Anderhuber F.** Waldeyer - Anatomie des Menschen. Berlin: De Gruyter, 2009, p. 954-957.

[2] **Juza, R.M. et al.** Clinical and surgical anatomy of the liver: A review for clinicians. Clinical Anatomy, 2014, 27(5), p. 764-769.

[3] **Lüllmann-Rauch, R. and Paulsen, F.** Taschenlehrbuch Histologie. Stuttgart: Thieme, 2012, p. 393-406.

[4] **Juza, R.M. et al.** Clinical and surgical anatomy of the liver: A review for clinicians. Clinical Anatomy, 2014, 27(5), p. 766.

[5] **Koolman, J. and Röhm, K.H.** Taschenatlas Biochemie des Menschen. Stuttgart: Thieme, 2009, p. 314-318.

[6] **Anthony, P.P. et al.** The morphology of cirrhosis. Recommendations on definition, nomenclature, and classification by a working group sponsored by the World Health Organization. Journal of clinical pathology, 1978, 31(5), p.395-414.

[7] **MacSween, R.N. et al.** Pathology of the liver. London: Churchill Livingstone, 2003, p. 575-620.

[8] **Bellentani, S. et al.** Prevalence of chronic liver disease in the general population of northern Italy: the Dionysos Study. Hepatology, 1994, 20(6), p. 1442-1449.

[13] **Trépo, C. et al.** Hepatitis B virus infection. The Lancet, 2014, 384(9959), p. 2053-2063.

[10] **Zachou, K. et al.** Review article: Autoimmune hepatitis - Current management and challenges. Alimentary Pharmacology and Therapeutics, 2013, 38(8), p. 887-913.

[11] **Bettermann, K. et al.** Steatosis and steatohepatitis: Complex disorders. International Journal of Molecular Sciences, 2014, 15(6), p. 9924-9944.

[12] **Farrell, G.C. et al.** Nonalcoholic fatty liver disease: From steatosis to cirrhosis. Hepatology, 2006, 43(1), p. 99-112.

[13] **MacSween, R. N.** Pathology of the liver. London: Churchill Livingstone, 2003, p.278-280.

[14] **Anthony, P.P. et al.** The morphology of cirrhosis. Recommendations on definition, nomenclature, and classification by a working group sponsored by the World Health Organization. Journal of clinical pathology, 1978, 31(5), p.395-414.

[15] **MacSween, R. N.** Pathology of the liver. London: Churchill Livingstone, 2003, p. 577-584.

[16] **MacSween, R. N.** Pathology of the liver. London: Churchill Livingstone, 2003, p. 595-604.

[17] **Herold, G.** Innere Medizin. Eine vorlesungsorientierte Darstellung. Köln: Eigenverlag Gerd Herold, 2015, p. 553-555.

[18] **Peng, Y.** Child-Pugh Versus MELD Score for Assessment of Prognosis in Liver Cirrhosis: A systhematic Review and Meta-Analysis of Observational studies. Medicine, 2016, 95(8), p. 1-29.

[19] **Herold, G.** Innere Medizin. Eine vorlesungsorientierte Darstellung. Köln: Eigenverlag Gerd Herold, 2016, p. 549-551.

[20] **Anon.** EASL-EORTC Clinical Practice Guidelines: Management of hepatocellular carcinoma. Journal of Hepatology, 2012, 56(4), p. 908-943.

[21] **Bosman, F.T. et al.** WHO Classification of Tumors of the Digestive System, 7th edition. Lyon: WHO IARC, 2010, p. 205.

[22] **El-Serag, H.B. et al.** Rising incidence of hepatocellular carcinoma in the United States. New England Journal of Medicine, 1999, 340(10), p. 745-750.

[23] **Hsu, I.C. et al**. Mutational hotspot in the p53 gene in human hepatocellular carcinomas. Nature, 1991, 350, p. 427-428.

[24] **El-Serag, H.B. et al.** Hepatocellular Carcinoma: Epidemiology and Molecular Carcinogenesis. Gastroenterology, 2007, 132(7), p. 2557-2576.

[25] **Clayton, E.F. et al.** Liver transplantation and cirrhotomimetic hepatocellular carcinoma: classification and outcomes. Liver transplantation, 2014, 20(7), p. 765-775.

[26] **Bosman, F.T. et al.** WHO Classification of Tumours of the Digestive System. Lyon: WHO IARC, 2010, p. 208-209.

[27] **Böcker, W. and Denk, H.** Pathologie. München: Elsevier, Urban und Fischer, 2012, p. 811-814.

[28] **Oikawa, T. et al.** Multistep and multicentric development of hepatocellular carcinoma: Histological analysis of 980 resected nodules. Journal of Hepatology, 2005, 42(2), p. 225-229.

[29] **Bosman, F.T. et al.** WHO Classification of Tumours of the Digestive System. Lyon: WHO IARC, 2010, p. 209-2011

[30] **Böcker, W. and Denk, H.** Pathologie. München: Elsevier, Urban und Fischer, 2012, p. 811.

[31] **MacSween, R. N.** Pathology of the liver. London: Churchill Livingstone, 2003, p. 577-584.

[32] **Bosman, F.T. et al.** WHO Classification of Tumours of the Digestive System. Lyon: WHO IARC, 2010, p. 728-730.

[33] Llovet, J.M. et.al. The Barcelona approach: diagnosis, staging, and treatment of hepatocellular carcinoma. Liver transplantation, 2004, 10(1), p. 115-120.

[34] **Pons, F. et al.** Staging systems in hepatocellular carcinoma. The Official Journal of the International Hepato Pancreato Biliary Association, 2005, 7(1), p. 35–41.

[35] **Kinoshita, A. et. al.** Staging systems for hepatocellular carcinoma: Current status and future perspectives. World Journal of Hepatology, 2015, 7(3), p. 406–424.

[36] **Yau, T. et al.** Evolution of systemic therapy of advanced hepatocellular carcinoma. World Journal of Gastroenterology, 2008, 14(42), p. 6437.

[37] **Anon.** EASL-EORTC Clinical Practice Guidelines: Management of hepatocellular carcinoma. Journal of Hepatology, 2012, 56(4), p. 908-943.

[38] **Xiang, Q. et al.** Tivantinib induces G2/M arrest and apoptosis by disrupting tubulin polymerization in hepatocellular carcinoma. Journal of experimental & clinical cancer research, 2015, 34, p. 118-131.

[39] **Katayama, R. et al.** Cytotoxic activity of tivantinib (ARQ 197) is not due solely to c-MET inhibition. Cancer Research, 73(10), 2013, p. 3087-3096.

[40] **Sin, J.E. et al.** Molecular targeted therapy for Hepatocellular Carcinoma: Current and future. World Journal of Gastroenterology, 2015, 19(37), p. 6144-6155.

[41] **Anon.** EASL-EORTC Clinical Practice Guidelines: Management of hepatocellular carcinoma. Journal of Hepatology, 2012, 56(4), p. 908-943.

[42] **Llovet, J.M. et al.** Sorafenib in advanced hepatocellular carcinoma. The New England journal of medicine, 2008, 359(4), p. 378-390.

[43] **So, B.J. et al.** Complete clinical response of metastatic hepatocellular carcinoma to sorafenib in a patient with hemochromatosis: a case report. Journal of hematology & oncology, 2008, 1, p.1-3.

[44] **Inuzuka, T. et al.** Complete response of advanced hepatocellular carcinoma with multiple lung metastases treated with sorafenib: A case report. Oncology, 2011, 81(1), p. 152-157.

[45] **Bladt, F. et al.** The c-Met Inhibitor MSC2156119J Effectively Inhibits Tumor Growth in Liver Cancer Models. Cancers, 2014, 6(3), p. 1736-1752.

[46] **Yan, B. et al.** Identification of MET genomic amplification, protein expression and alternative splice isoforms in neuroblastomas. Journal of Clinical Pathology, 2013, 66(11), p. 985-991.

[47] **Weinberg, R.A. et al.** CST Guide: Pathways & Protocols. First edition. Danvers, MA: CST. p. 42-48.

[48] **Lipika, G. et al.** Targeting the HGF/c-MET pathway in hepatocellular carcinoma. Clinical Cancer Research, 2013, 19(9), p. 2310-2318.

[49] **Raghav, K.P. et al.** Role of HGF/MET axis in resistance of lung cancer to contemporary management. Translational lung cancer research, 2012, 1(3), p. 179-193.

[50] **Kondo, S. et al.** Clinical impact of c-Met expression and its gene amplification in hepatocellular carcinoma. International Journal of Clinical Oncology, 2013, 18(2), p. 207-213.

[51] **Lee, S.J. et al.** A Survey of c-MET Expression and Amplification in 287 Patients with Hepatocellular Carcinoma. Anticancer Research, 2013, 33(11), p. 5179-5186.

[52] **Wu, F. et al.** The clinical value of hepatocyte growth factor and its receptor c-met for liver cancer patients with hepatectomy. Digestive and liver disease, 2006, 38(7), p. 490-497.

[53] **Pecchi, A. et al.** Post-transplantation hepatocellular carcinoma recurrence: Patterns and relation between vascularity and differentiation degree. World Journal of Hepatology, 2015, 7(2), p. 276-284.

[54] **Scaggiante, B. et al.** Novel hepatocellular carcinoma molecules with prognostic and therapeutic potentials. World Journal of Gastroenterology, 2014, 20, p. 1268-1288.

[55] **Gao, J.J. et al.** Sorafenib-based combined molecule targeting in treatment of hepatocellular carcinoma. World Journal of Gastroenterology, 2015, 21(42), p. 2059-2070.

[56] **Ebos, J.M. et al.** Tumor and host-mediated pathways of resistance and disease progression in response to antiangiogenic therapy. Clinical Cancer Research, 2009, 15, p. 5020–5025.

[57] **Scaggiante, B. et al.** Novel hepatocellular carcinoma molecules with prognostic and therapeutic potentials. World Journal of Gastoenterology, 2014, 20(5), p. 1268-1288.

[58] **Giordano, S. et al.** Met as a therapeutic target in HCC: Facts and hopes. Journal of Hepatology, 60(2), 2014, p.442-452.

[59] **Karagonlar, F.Z. et al.** Elevated hepatocyte growth factor expression as an autocrine c-Met activation mechanism in acquired resistance to sorafenib in hepatocellular carcinoma cells. Cancer Science, 2016, 107(4), p. 407-416.

[60] **Chen, W. et al.** Hepatic stellate cell coculture enables sorafenib resistance in Huh7 cells through HGF/c-Met/Akt and Jak2/Stat3 pathways. BioMed Research International, 2014, 1, p. 1-10.

[61] **Miller, B. et al.** Reporting results of cancer treatment. Cancer, 1981, 47(1), p. 207-214.

[62] **Duffaud, F. et al.** New guidelines to evaluate the response to treatment in solid tumors. Bulletin du cancer, 2000, 87(12), p. 881-886.

[63] Lencioni, R. et al. Modified RECIST (mRECIST) Assessment for Hepatocellular Carcinoma. Seminars in Liver Disease, 2010, 212, p. 52-60.

[64] **Thavarajah, R. et al.** Chemical and Physical Basics of Routine Formaldehyde Fixation. Journal of Oral and Maxillofacial Pathology, 2012, 16(3), p. 400-405.

[62] **Jubb, A. et al.** Quantitative analysis of colorectal tissue microarrays by immunofluorescence and in situ hybridization. Journal of pathology, 2003, 200, p. 577-588.

[66] **Böcker, W. and Denk, H.** Pathologie. München: Elsevier, Urban und Fischer, 2012, p. 42.

[67] **Wang, F. et al.** RNAscope: A Novel In Situ RNA Analysis Platform for Formalin-Fixed Paraffin-Embedded Tissues. Journal of Molecular Diagnostics, 2012, 14(1), p. 22-29.

[68] **Price, E.R. et al.** Human cyclophilin B: a second cyclophilin gene encodes a peptidyl-prolyl isomerase with a signal sequence. Proceedings of the National Academy of Sciences of the United States of America, 1991, 88(5), p.1903-1907.

[69] **Lu, Y. et al.** Alpha fetoprotein plays a critical role in promoting metastasis of hepatocellular carcinoma cells. Journal of Cellular and Molecular Medicine, 2016, 20, p. 549–558.

[70] **Neuzillet, C. et al**. High c-Met expression in stage I–II pancreatic adenocarcinoma: proposal for an immunostaining scoring method and correlation with poor prognosis. Histopathology, 2015, 67, p. 664-676.

[71] **Helin, H.O. et al.** Free digital image analysis software helps to resolve equivocal scores in HER2 immunohistochemistry. Virchows archiv, 2016, 468(2), p. 191-198.